US Army Corps of Engineers

GEOTECHNICAL LABORATORY

TECHNICAL REPORT GL-91-23

A STUDY OF EMBANKMENT PERFORMANCE DURING OVERTOPPING

by

Paul A. Gilbert, S. Paul Miller

Geotechnical Laboratory

DEPARTMENT OF THE ARMY
Waterways Experiment Station, Corps of Engineers
3909 Halls Ferry Road, Vicksburg, Mississippi 39180-6199

November 1991

Final Report

Prepared for DEPARTMENT OF THE ARMY
US Army Corps of Engineers
Washington, DC 20314-1000

Under CWIS Work Unit 81710

REPORT DOCUMENTATION PAGE

Form Approved
OMB No. 0704-0188

1. AGENCY USE ONLY *(Leave blank)*

2. REPORT DATE
November 1991

3. REPORT TYPE AND DATES COVERED
Final report, Oct 1981-April 1989

4. TITLE AND SUBTITLE
A Study of Embankment Performance During Overtopping

5. FUNDING NUMBERS
CWIS Work Unit 81710

6. AUTHOR(S)
Gilbert, Paul A.; Miller, S. Paul

7. PERFORMING ORGANIZATION NAME(S) AND ADDRESS(ES)
USAE Waterways Experiment Station
Geotechnical Laboratory, 3909 Halls Ferry Road
Vicksburg, MS 39180-6199

8. PERFORMING ORGANIZATION REPORT NUMBER
Technical Report GL-91-23

9. SPONSORING/MONITORING AGENCY NAME(S) AND ADDRESS(ES)
US Army Corps of Engineers
Washington, DC 20314-1000

10. SPONSORING/MONITORING AGENCY REPORT NUMBER

11. SUPPLEMENTARY NOTES
Available from National Technical Information Service, 5285 Port Royal Road, Springfield, VA 22161

12a. DISTRIBUTION/AVAILABILITY STATEMENT
Approved for public release; distribution is unlimited.

12b. DISTRIBUTION CODE

13. ABSTRACT *(Maximum 200 words)*

A study was undertaken to determine how embankments behave when overtopped and, based on this knowledge, to predict overtopping performance of different types of embankments (earthen, rock fill, etc.) and to recommend defensive measures that would increase the durability of an overtopped embankment. An experience-oriented approach was taken. Pertinent literature was reviewed. Prototype dams subjected to overtopping, centrifuge modeling of overtopping embankments, and numerical modeling techniques are described.

14. SUBJECT TERMS
See reverse.

15. NUMBER OF PAGES
100

16. PRICE CODE

17. SECURITY CLASSIFICATION OF REPORT	18. SECURITY CLASSIFICATION OF THIS PAGE	19. SECURITY CLASSIFICATION OF ABSTRACT	20. LIMITATION OF ABSTRACT
UNCLASSIFIED	UNCLASSIFIED	UNCLASSIFIED	

14. (Continued).

Breach
Centrifuge modeling of embankments
Embankments
Flume modeling
Mathematical models of embankments
Overtopping

PREFACE

This report, prepared by the Geotechnical Laboratory (GL) of the US Army Engineer Waterways Experiment Station (WES), describes work done under CWIS Work Unit No. 81710, "Failure Mechanisms in Earth and Rockfills Under Critical Flow Conditions," for Headquarters, US Army Corps of Engineers, during the period October 1981 to April 1989. The report was written by Messrs. Paul A. Gilbert and S. Paul Miller of the Soils Research Facility (SRF) and Engineering Group (EG), respectively, under the supervision of Messrs. Gene P. Hale and Gerald B. Mitchell, Chief, SRF and EG, respectively, Mr. Clifford B. McAnear, Chief, Soil Mechanics Division, and Dr. William F. Marcuson III, Chief, GL.

Technical reviews were provided by Messrs. Noel R. Oswalt, Chief, Spillways and Channels Branch, Hydraulic Structures Division, Hydraulics Laboratory (HL), and William A. Thomas, Waterways Division, HL. Their contribution to this work is greatly appreciated.

Commander and Director of WES during the preparation of this report was COL Larry B. Fulton, EN. Technical Director was Dr. Robert W. Whalin.

CONTENTS

CONVERSION FACTORS, NON-SI TO SI (METRIC) UNITS OF MEASUREMENT

Non-SI units of measurement used in this report can be converted to SI (metric) units as follows:

Multiply	By	To Obtain
acre-feet	1.233489	cubic kilometres
acres	4.046873	square kilometres
cubic feet	0.02831685	cubic metres
cubic feet per second	0.02831685	cubic metres per second
degrees (angle)	0.01745329	radians
feet	0.3048	metres
inches	2.54	centimetres
ounces (mass)	28.34952	grams
tons (short)	907.1847	kilograms

A STUDY OF EMBANKMENT PERFORMANCE DURING OVERTOPPING

PART I: INTRODUCTION

Background

1. Overtopping of Corps of Engineers (CE) cofferdams, partially complete embankments, and levees has caused expensive damage, construction delays, and threats to downstream life and property. Studies of earth dam failures have indicated, in fact, that 40 percent of the dams which fail do so as the result of overtopping (Linsley and Franzini 1979). Therefore, it follows that earthen dams and other flood-control structures resistant to catastrophic erosion during overtopping can mitigate damage and substantially reduce risk to downstream life and property. Overtopping is generally due to the failure, inadequate size, or omission of outlet works and/or emergency spillway. Overtopping occurs as the result of increased water level which is caused by one of four mechanisms.

- a. Seiches in the reservoir. Seiches are long periods of oscillation of the surface of shallow inland bodies of water usually generated by wind. Variations in water level due to seiches have been observed to be as much as 8 ft.*
- b. Slides or rockfalls into the reservoir.
- c. Rainfall or snowmelt and consequent runoff into the reservoir.
- d. Upstream water release, e.g., an upstream embankment fails, releasing its reservoir.

Even though embankments are not designed to be overtopped, some earthen structures have been overtopped for relatively long periods without catastrophic failure. Conditions surrounding overtopping, however, are not conducive for evaluating embankment performance since an emergency situation usually exists during instances of overtopping with efforts more appropriately directed toward saving life and property. Additionally, because the types of structures with the highest risk of overtopping are cofferdams, levees, and older

* A table of factors for converting non-SI units of measurement to SI (metric) units is presented on page 4.

dams with poorly documented construction procedures, even basic mechanical properties of the embankment materials may be unknown.

2. Hydraulic dam breach analyses currently being made on CE dams are used to predict downstream flood stages. However, such analyses are significantly affected by dam failure mechanisms applied in the model, and because of the lack of a data base, arbitrary methods are presently being used to model dam failure. Actual outflows from a breached dam with time involve the complex interaction of many variables, some of which are difficult to quantify, such as the dimensions of the breach and how they change with time, volume and size of the reservoir, tailwater conditions, reservoir inflow, soil conditions, and other variables.

3. Realistic embankment failure prediction and resulting reservoir release will significantly improve estimates of downstream flood stages.

Purpose and Scope

4. This report describes a study undertaken to (a) determine how embankments behave when overtopped and (b) based on this knowledge, predict overtopping performance of embankment types (e.g., earthen, rock fill, etc.) and (c) recommend defensive measures which would increase the durability of an overtopped embankment. Since very little documentation or knowledge existed on this subject, an experience-oriented approach was taken. However, methods of mathematical modeling were reviewed and it was intended to pursue a numerical approach to the problem if warranted; as subsequently shown, it was not.

5. Additionally, previous modeling which might apply to embankment overtopping was studied as were principles of erosion and sediment transport. Because physical and fiscal constraints prevented normal physical modeling, centrifuge modeling for studying embankment performance during overtopping was evaluated. Developments from this study are reported herein.

PART II: PROTOTYPE EXPERIENCE

Overview

6. Interviews, record collection, and published literature provided information on overtopping. Because many of the case histories lacked important quantitative details, they were not reported here although they did provide background and many are listed in the references.

7. Prototype experiences are classified by embankment type into one of four categories.

- a. Earth and random fills.
- b. Rock fills with an impermeable element.
- c. Unreinforced rock fill with no impervious element.
- d. Reinforced rock fill.

Earth and random fills were the most common and would be expected to be most important in the future since this classification covers most cofferdams and levees, which are the embankments most frequently subjected to unplanned overtopping. Overtopped rock fills with an impermeable element generally were partially complete main embankments. Again, because of limited diversion capacity and the limited resistance to overtopping of cofferdams, partially complete embankments are particularly susceptible to damage by overtopping should the diversion system and cofferdam capacity be exceeded. Rock fills, unreinforced and without an impervious element, are rare; circumstances of the two overtoppings of this type were unique. Reinforced rock-fill dams are zoned structures in which the downstream slope is reinforced with a metal grid held in place by steel bars embedded into the embankment during construction. This reinforcement enhances the embankment's resistance to overtopping and contributes to the stability of the downstream slope. Reinforced rock fills have proven useful in several countries, particularly Australia and South Africa, but there is very little United States experience.

8. These prototype experiences with model results will provide the experience base for an hypothesis of embankment behavior during overtopping and proposed defensive measures which can increase embankment durability during overtopping.

Earth and Random Fills

9. Twenty-six examples are provided of overtopped earth and random fills. Several other overtopping events were reviewed but were excluded from the following discussion because quantitative data were unavailable.

Clarence Cannon coffer-
dam and main embankment

10. General description. Located near Hannibal, Missouri, on the Salt River, Clarence Cannon Dam is a concrete and earth-fill dam with a height of 138 ft and crest length of 1940 ft. In July of 1981, gates in the concrete section were being used for river diversion while a 45-ft-high random earth cofferdam protected the earth-fill portion of the dam. The partially complete main earth embankment, located about 900 ft downstream of the cofferdam, had a crest elevation 15 ft lower than the cofferdam crest (Figure 1). A horizontal drainage blanket underlying the downstream portion of the main embankment was connected to a vertical chimney drain which ran along the embankment center line. At the time of overtopping, the top of the chimney drain was covered by 3 ft of cohesive fill. The lower 37 ft of the cofferdam had 1V on 3H slopes, while the upper 8 ft had been placed at angle of repose (≈1V on 1H) and compacted by equipment traffic. When overtopping became imminent, a notch was made 400 ft along the cofferdam from the left abutment (Figure 2). Notch elevation was 5 ft below the cofferdam crest. Material in this area of the cofferdam was a stiff clay which would be resistant to erosion, and the location would divert most of the flow over the partially complete main embankment and away from the concrete structure.

11. Overtopping data. Date - 27-30 July 1981; maximum depth - 5 ft, duration - 3 days.

12. Damage. Overtopping flow was primarily contained in the notch area, with breaching in the center of the notch occurring after 20 hr of overtopping. Maximum depth (5 ft) was reached about this time. Limited flow over other areas of the cofferdam occurred for a few hours prior to notch breaching. The partially complete earth embankment, with very shallow slopes, allowed spread of the flow over a crest length of 850 ft. Apparently, the main embankment sustained very little damage until about 8 hr after notch breaching. At this time erosion reached the horizontal drainage blanket at the downstream main embankment toe and started removing the granular blanket

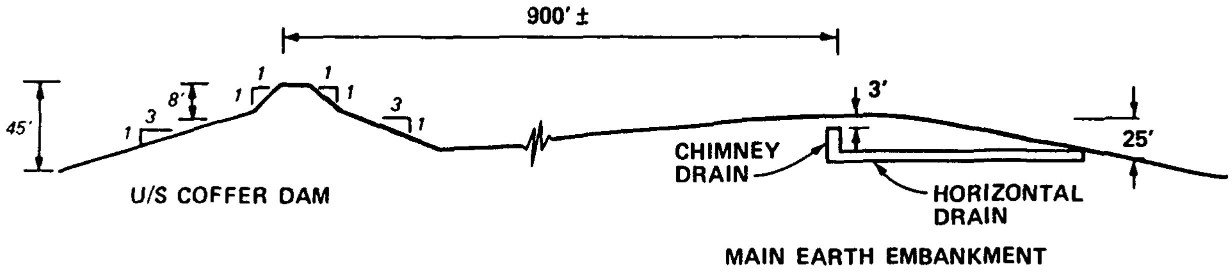

Figure 1. Clarence Cannon Dam - July 1981

Figure 2. Notch area of Clarence Cannon cofferdam during initial overtopping

materials from beneath the central portion of the downstream slope. Undercutting of the overlying cohesive fill by removal of the drainage blanket continued for 8 or 10 hr until the chimney drain was reached. The chimney drain was removed from the left abutment to the concrete dam section without appreciable damage to the upstream portion of the main embankment. The chimney drain and 30 to 40 percent of the downstream embankment fill were lost.

13. The cofferdam of cohesive soil (stiff clay) withstood 20 hr of overtopping at water depths up to 5 ft (upstream stage minus notch elevation). Tailwater, maintained within 8 to 10 ft of the notch crest, probably delayed removal of toe material and subsequent breaching. Control of the overtopping location was successful--the notch area probably provided the most durable and uniform performance compared to putting water over the whole cofferdam which had poorly compacted material in the upper 8 ft.

Bloomington Lake diversion cofferdam

14. General description. Sited on the North Branch of the Potomac River along the Maryland-Virginia border, two diversion structures for Bloomington Dam were overtopped in 1978. An upstream diversion dike, approximately 30 ft high, provided initial diversion of the river while a diversion cofferdam was being constructed approximately 400 ft downstream. The diversion cofferdam was a random earth (clayey sandy gravel) fill with an upstream impervious blanket and cutoff and a downstream rock toe filter (Figure 3). The earth fill specification limited maximum size to 8 in., with 20 percent or more passing the No. 200 sieve, and required 12-in. loose lifts compacted by a 50-ton rubber tired roller. With upstream slopes of 1V on 3H and downstream slopes of 1V on 2.5H, the cofferdam's upstream 30 ft of crest had been completed to an elevation 4 ft above the dike crest (el 1270) while the downstream 70 ft was at a level 2 ft below dike crest.

15. Overtopping data. Date - 3 July 1978; maximum depth - 5 ft; duration - unknown (10 hr before breaching).

16. Damage. Floodwaters overtopped the dike for about 25 min before the cofferdam was overtopped. After 4 hr of overtopping, erosion began adjacent to the right abutment which was lower than the rest of the embankment. The erosion continued through the cofferdam until full breaching occurred approximately 10 hr after overtopping started (Figures 4 and 5). The breach was 70 ft wide and eroded to foundation level with vertical faces. The remaining portion of the embankment's downstream slopes had vertical faces

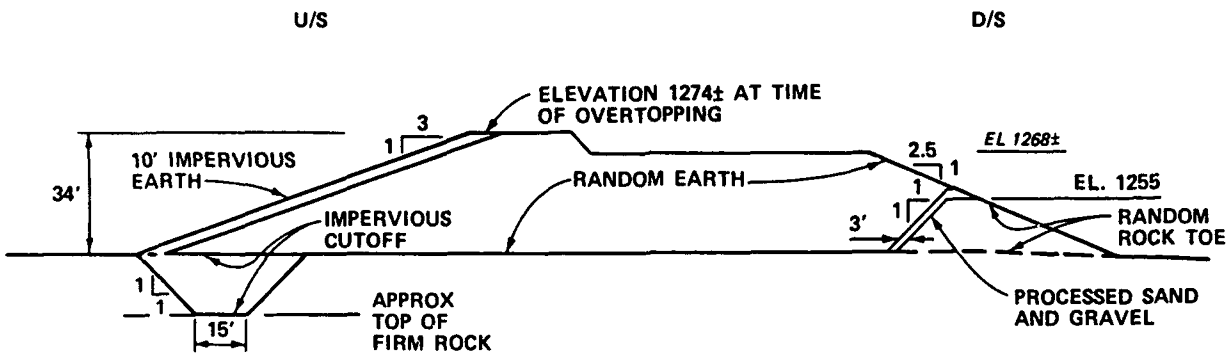

Figure 3. Bloomington Lake diversion cofferdam

15 to 20 ft high. Breaching of the diversion dike followed cofferdam breaching by 10 min.

17. Breaching, which occurred at the lower part of the embankment and at the more abrupt (right) abutment, took 4 hr to start and 10 hr to complete. The relatively long crest (± 100 ft) increased breaching time. The more easily eroded rock toe probably accelerated undercutting of the downstream slope and subsequent breaching. Other factors possibly accelerating breaching were concentration of flow at the right abutment and poor fill/abutment contact there. A homogeneous (no granular components) random earth fill composed of fine-grained compacted soil would have withstood overtopping longer, especially in light of the long crest length. If the left portion of the embankment had been lower and received the major portion of flow, breaching might have been delayed further because of the shallow, sloped left abutment. This would have provided a large earth mass for erosion.

18. The dike upstream of the cofferdam likely suffered quick failure due to rapid loss of tailwater and saturation of the downstream slope.

R. D. Bailey permanent
<u>cofferdam and diversion structure</u>

19. <u>General description.</u> Located on the Guyandot River in southern West Virginia, the R. D. Bailey Dam is a 310-ft-high, 1200-ft-long rock-fill dam with an upstream reinforced concrete membrane. During the construction period, the main dam construction was protected by two upstream structures. These were (a) an upstream diversion structure, consisting of seven 60-ft-diam sheet pile cells with an embankment portion at the right abutment, and (b) a porous sandstone permanent cofferdam which would serve as the upstream toe of the main dam. Both were overtopped. The 60-ft-high diversion structure,

Figure 4. Breach of Bloomington Lake cofferdam

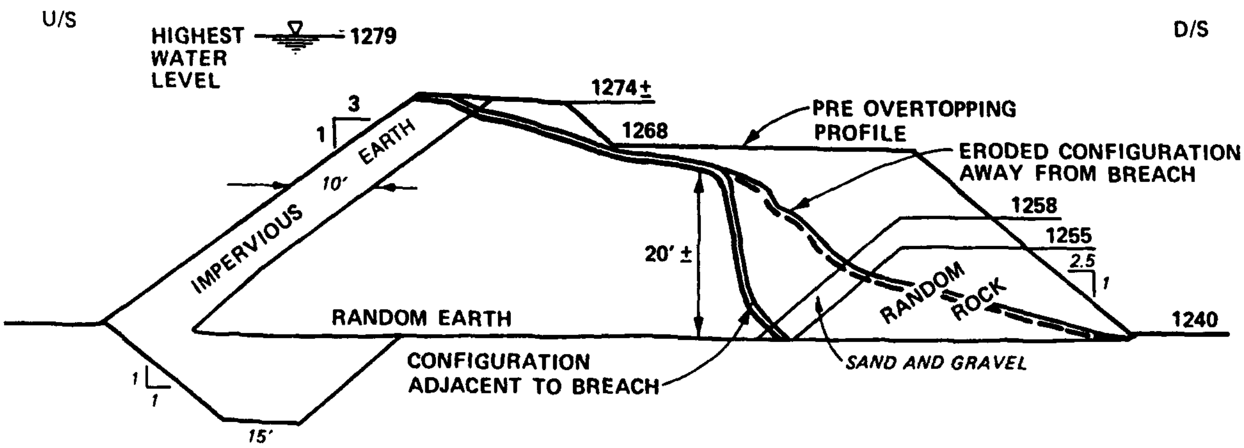

Figure 5. Bloomington Lake diversion cofferdam after failure

located about 70 ft upstream of the permanent cofferdam, had a rock-fill downstream slope, 1V on 2H, covered with 3 in. of shotcrete. The partially complete, permanent cofferdam (Figure 6) consisted of well graded sandstone compacted by rollers in 24-in. lifts and had slopes of 1V on 2H upstream, 1V on 1.5H downstream. A 160-ft notch had been excavated in the permanent cofferdam along the crest at the left abutment. With a crest width (upstream to downstream) of approximately 400 ft, the notch crest had the same elevation as the diversion structure, 950 ft msl. The purpose of the notch was to permit flood passage without impounding water higher than the diversion structure.

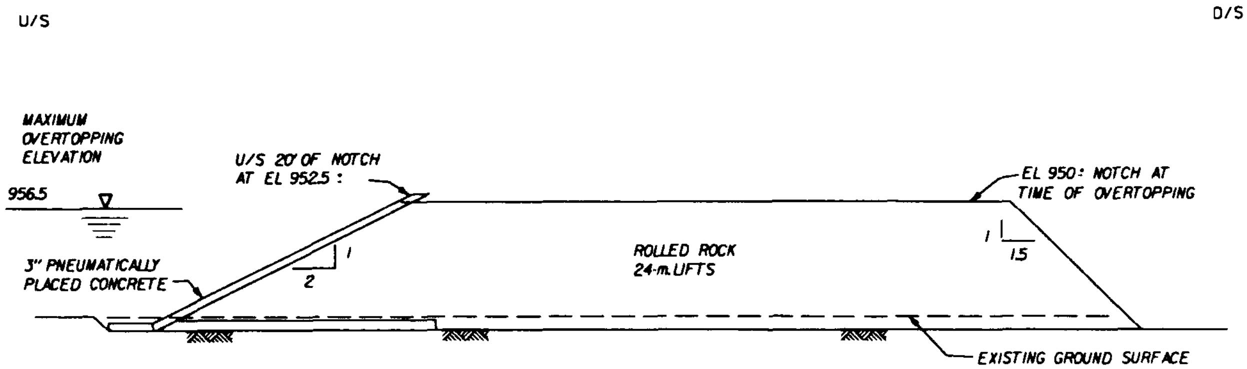

Figure 6. R. D. Bailey permanent cofferdam section through notch

20. Overtopping data. Date - 14 March 1975; maximum depth - 6.5 ft; duration - ± 24 hr.

21. Damage. Breaching reached the upstream slope 4 hr after the start of overtopping, about the same time as maximum depth of overtopping. Figures 7a and 7b show notch erosion as breaching moved upstream. Subsequent lateral and downward erosion enlarged the breach to a width of 70 ft and to a level within 5 ft of the foundation (Figures 8 and 9). Once the water elevation started dropping between the diversion structure and the permanent cofferdam, erosion of the berm downstream of the cells was noted (Figure 10). This erosion continued for about an hour, and stabilized at a level 30 ft below the sheet pile cell elevation.

22. The downstream berm of the diversion structure had been repaired to a 1V on 3H slope with a downstream toe of derrick stone (2- to 4-ft size), when a second overtopping occurred on 20 March 1975. This overtopping lasted for 15 hr, with a maximum depth of 2.5 ft, and caused erosion of the berm to the same level as the 14 March overtopping. Following this event, the berm

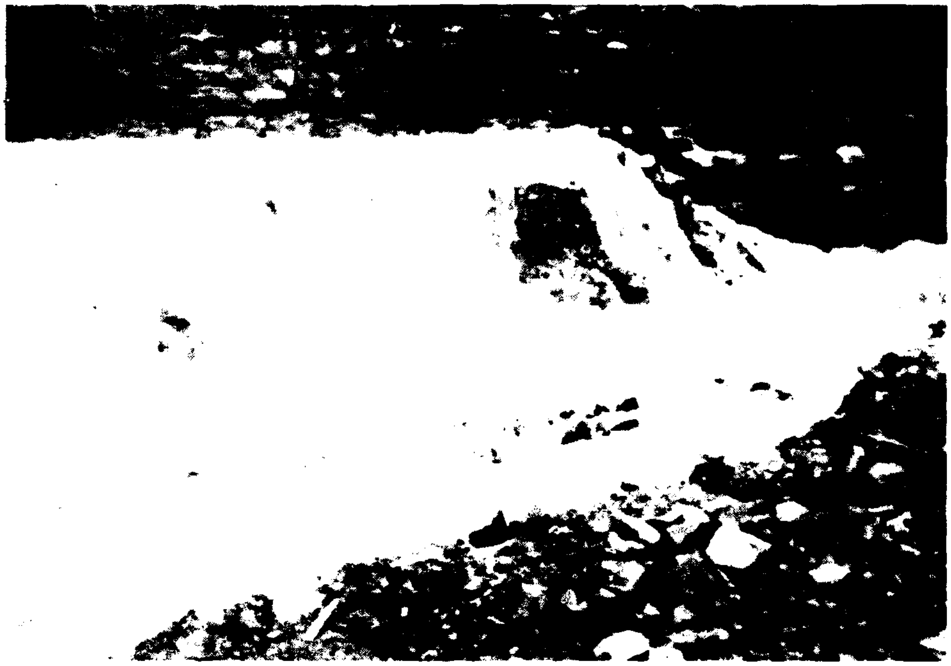

a. Early erosion

b. Terminal erosion

Figure 7. Breaching erosion of R. D. Bailey cofferdam

Figure 8. Breach of R. D. Bailey cofferdam looking upstream

Figure 9. Breach of R. D. Bailey cofferdam looking downstream

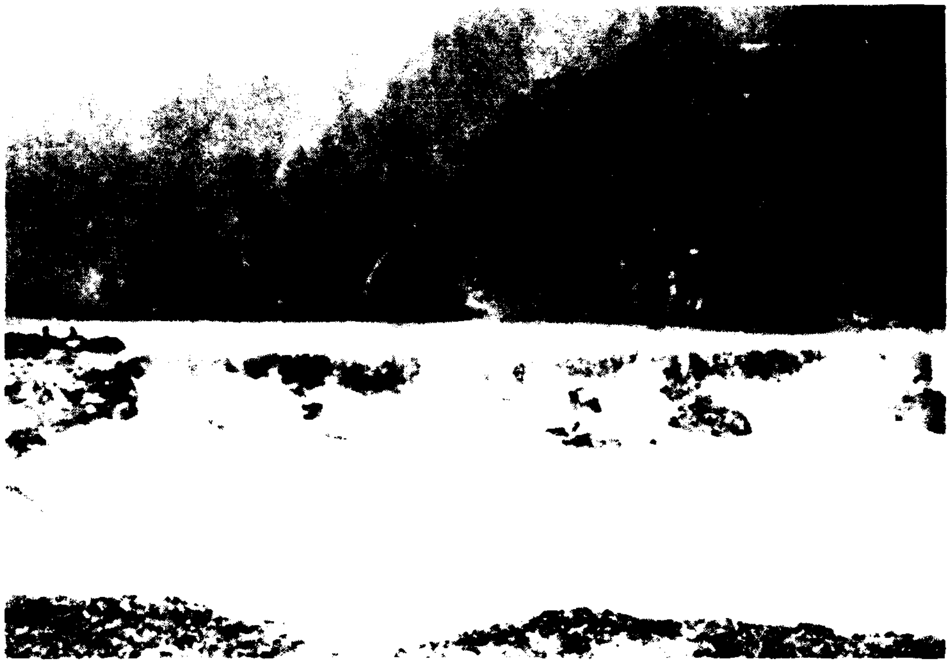

Figure 10. Berm erosion on downstream side of cellular cofferdam at R. D. Bailey Dam

was restored to the 1V on 3H slope, with a splash pad at an elevation 15 ft below the structure crest. Twelve inches of concrete was placed over the berm with reinforced concrete on the splash pad. On 30 March 1974, a third overtopping, lasting 24 hr, with a maximum crest of 3 ft caused minimal damage to the berm area. The permanent cofferdam breach was left open during the 20 and 30 March events.

23. Breaching took a relatively short time to reach the upstream slope compared to the Bloomington experience. The pneumatically placed concrete on the upstream slope likely delayed or minimized seepage flow through the embankment until overtopping occurred. This, in turn, probably delayed instability and movement of the downstream slope due to seepage forces. Rather extensive protection of the downstream slope of the sheet pile diversion structure successfully protected the structure during a subsequent overtopping of comparable magnitude.

Elm Fork Structure 9

24. General description. One of a large number of Soil Conservation Service (SCS), US Department of Agriculture (USDA) flood-retarding structures, Elm Fork Structure 9 is a 35-ft-high clay embankment consisting of CL clay

with some CH material near Gainesville in north-central Texas (USDA 1983). The downstream slope of the well sodded dam was 1V on 2H.

25. Overtopping data. Date - 12 October 1981; maximum depth - 0.4 ft; duration - ±3 hr.

26. Damage. Figure 11 is a general view of the damaged embankment; Figures 12a and 12b provide a closer view of the damaged downstream slope. The overtopping caused gullies or rills up to 5 ft in depth in the downstream slope. Apparently the overtopping lasted long enough to strip the vegetative topsoil and root structure from the compacted embankment layers along most of the embankment.

Figure 11. General view of Elm Fork Structure 9

Colorado flood-retarding structures

27. General description. The embankments, similar to Elm Fork Structure 9, located in southeastern Colorado, were overtopped in June 1965 (Mitchell, King, and Rallison 1966). The three embankments, known as M-1, S-1, and W-1, had the same general soil composition, SC to CL, and slopes, 3H on 1V upstream and 2-1/2H on 1V downstream. Embankment heights were: M-1, 38 ft; S-1, 25 ft; and W-1, 47 ft. The report noted that M-1 had good grass cover.

a.

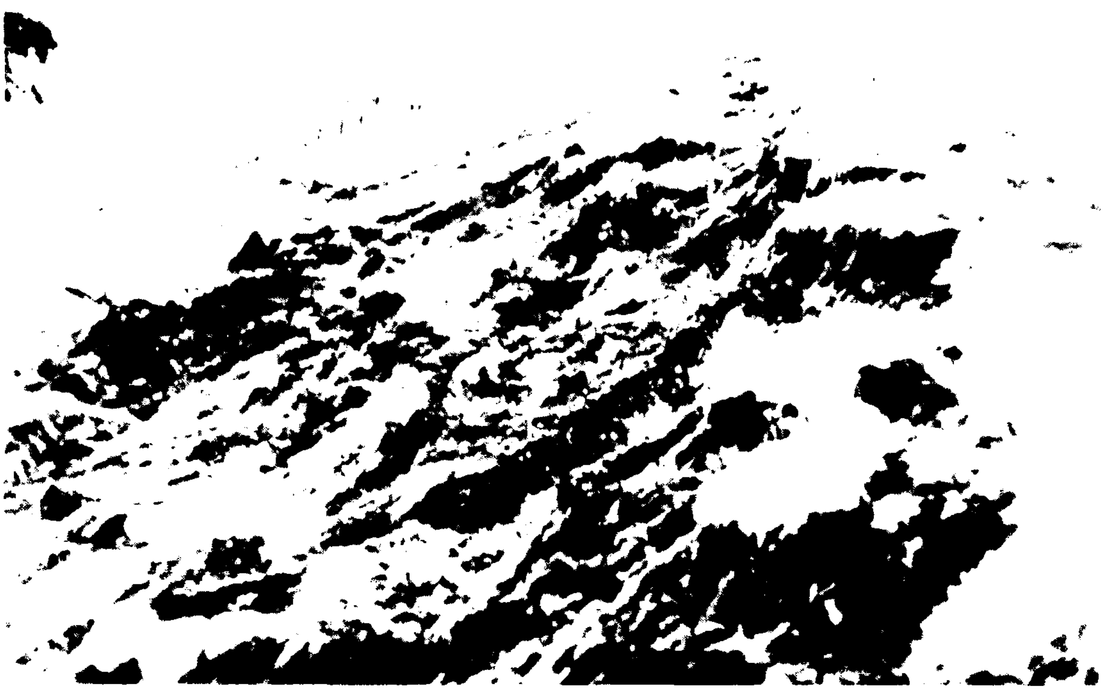

b.

Figure 12. Downstream slope damage of Elm Fork Structure 9

28. Overtopping data.

a. M-1: Date - 16 or 17 June 1965; maximum depth - 1 ft; duration - 2 to 4 hr.

b. S-1: Date - 16 or 17 June 1965; maximum depth - 0.75 ft; duration - 2.4 hr.

c. W-1: Date - 16 or 17 June 1975; maximum depth - 2.5 ft; duration - 1 to 2 hr.

29. Damage. W-1, considered moderately damaged, had erosion on the downstream slope and some head cutting at the right abutment but did not breach. S-1 and M-1 had only minor damage. Deepest overtopping occurred over portions of the embankments nearest the abutments. The embankments, designed with a longitudinal crown over the highest portion of the embankment, still had a crown due to smaller than expected settlements.

Upper Elk River and Big Caney watershed embankments

30. General description. Three embankments in the Upper Elk River watershed and one of the Big Caney watershed embankments, southeastern Kansas, were overtopped in July 1976 (Anon 1976). Again, these dams were similar to Elm Fork Structure 9 and the Colorado flood-retarding structures. The Upper Elk River and Big Caney structures had the following characteristics:

Structure	Soil	Height ft	Slopes U/S	Slopes D/S
Upper Elk River 37	CL with some GC	45	3H on 1V	2-1/2H on 1V
Upper Elk River 41	CL with some GC	45	3H on 1V	2-1/2H on 1V
Upper Elk River 42	CL with some GC	39	3H on 1V	2-1/2H on 1V
Big Caney 39	CL with some GC	41	3H on 1V	2-1/2H on 1V

31. Overtopping data.

a. Upper Elk River 37: Date - 2-3 July 1976; maximum depth - 2.5 ft; duration - unknown.

b. Upper Elk River 41: Date - 2-3 July 1976; maximum depth - 1.8 ft; duration - unknown.

c. Upper Elk River 42: Date - 2-3 July 1976; maximum depth - 1.0 ft; duration - 0.5 hr.

d. Big Caney 39: Date - 2-3 July 1976; maximum depth - 0.3 ft; duration - unknown.

32. Damage. Damage to Upper Elk River 41 and 42 and Big Caney 39 was considered minor. Upper Elk River 37, with good vegetative cover, suffered more extensive but minor damage (Figures 13a and 13b). The outer cover of the

a.

b.

Figure 13. Downstream slope damage of Upper Elk River 37

embankments was a 1-ft vertical depth of loosely compacted topsoil to support vegetation. Apparently this looser material along with the grass and its root mass was the first material removed at several points along the embankment (Figure 14).

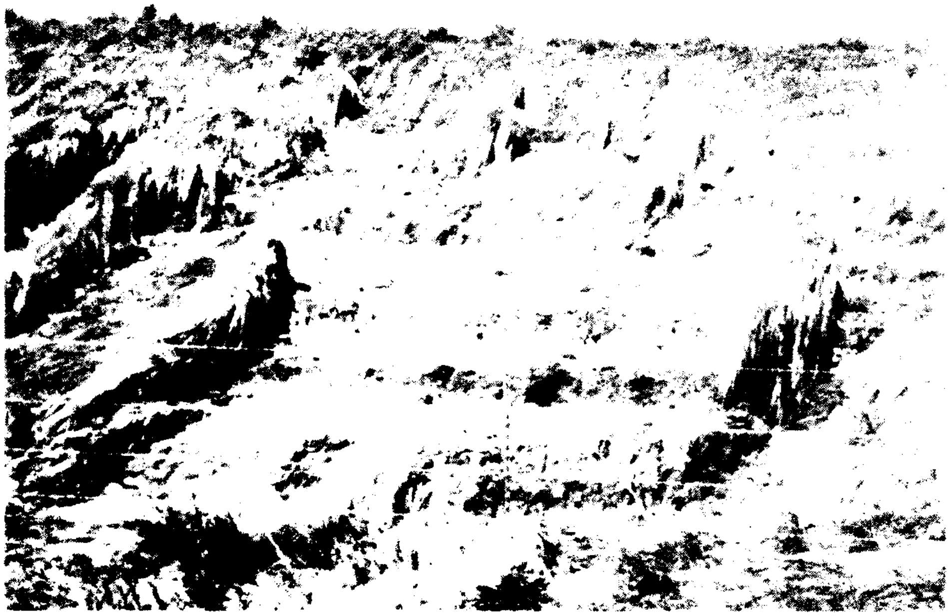

Figure 14. Closeup of downstream slope damage to Upper Elk River 37

Oros Dam, Brazil

33. General description. A zoned earth and rock fill embankment with a clay core completed to a height of 30 m, Oros Dam was overtopped in March 1960 (Wustemann 1960 and Budweg 1982). The dam has a circular alignment between two abutments at an acute angle. At the time of overtopping the clay core (LL = 27, PL = 17) with a 100-m base was the highest component of the dam. Compacted sand and tipped rock zones either side of the core were at core level upstream and 5 m lower downstream. The clay core was raised 5 m with uncompacted fill just prior to overtopping. A breach was prepared once overtopping became certain, and aircraft dropped metal sheeting on the dam in an attempt to protect it from erosion.

34. Overtopping data. Date - 25-26 March 1960; maximum depth - 2.7 ft (0.8m); duration - 12 hr (before major damage).

35. Damage. Breaching took place after 12 hr in the central portion of the dam. After approximately another 6 hr, the breach widened to 150 to 200 m. A large amount of water rather quickly passed through the breach

causing a flood wave to move downstream. The remaining embankment was eroded, particularly at the abutments.

Euclides de Cumba Dam, Brazil

36. General description. A 63-m-high homogeneous earth fill with a curved axis, a vertical sand drain, and bermed, grassy downstream slope, Euclides de Cumba Dam is located on the Prado River (Anon 1977 and Budweg 1982).

37. Overtopping data. Date - 19-20 January 1977; maximum depth - 1.26 m; duration-7.5 hr (before breaching began).

38. Damage. The downstream slope suffered severe erosion before breaching occurred. Removing about one third of the embankment, overtopping water eroded the downstream slope rather uniformly. The breach occurred at the right abutment, removing about one third of the 310-m-long embankment.

Armando de Salles Oliveira Dam, Brazil

39. General description. Located 10 km downstream of Euclides de Cumba Dam, Armando de Salles Oliveira Dam is 660 m long with two 35-m-high homogeneous earth fills of rolled clay with inclined and horizontal drains (Anon 1977 and Budweg 1982).

40. Overtopping data. Date - 20 January 1977; maximum depth - 1.3 m; duration - 15 to 30 min.

41. Damage. When the Euclides de Cumba Dam began breaching, a flood wave formed which overtopped and failed the Armando de Salles Oliveira Dam 15 to 30 min later. Breaching occurred at the right abutment of the right embankment and through a low saddle embankment on the reservoir rim. Outside the breached areas, there was very little damage to the downstream slope. Approximately one third of the right embankment volume was removed.

Little Blue River levees, Missouri

42. General description. Levees along the Little Blue River (MRLS R-351), a tributary of the Missouri River east of Kansas City, Missouri, were overtopped in 11 places during September 1977 (Figure 15). Approximately 15 ft high with slopes of 1V on 3H, the embankments were generally composed of clay soil (LL = 40, PI = 22) with good vegetation. These levees were overtopped again in August 1982.

43. Overtopping data. Dates - 13 September 1977 and 13-14 August 1982; maximum depths - 1 ft and 0.7 to 0.9 ft; durations - 12 hr and 20 hr.

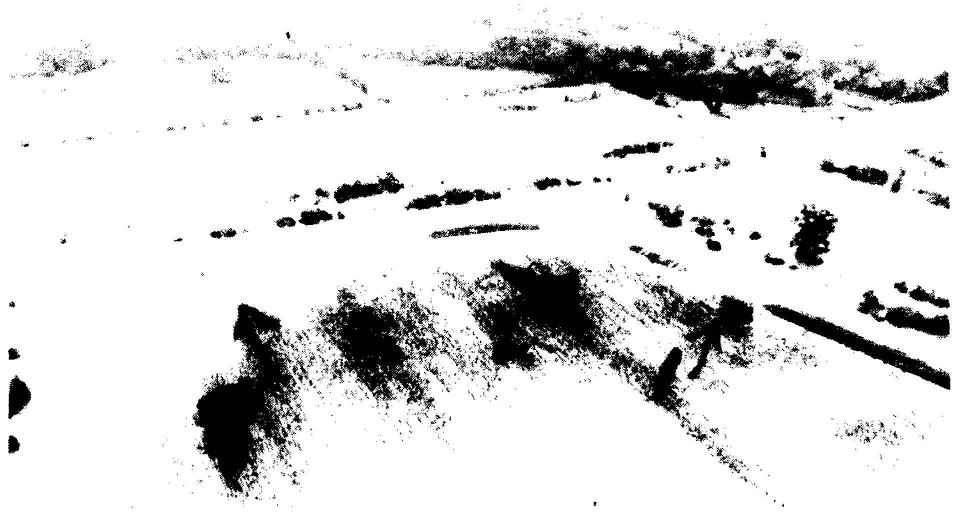

Figure 15. View of Little Blue River overtoppings

44. Damage. For the 1977 overtopping, levee damage consisted of road gravel washed from the crest to the downstream slope, a landside scour hole, and rill erosion. Breaching did not occur. The levees were previously overbuilt with silty materials due to stability problems, and these areas were more severely damaged with scour holes and gully formation. These areas did not support a good stand of grass as did the clayey areas.

45. In 1982, the overtopping occurred over some of the same levee, but sometime after 12 hr of overtopping flow, breaching occurred in a well vegetated portion of the levee.

Jacksonport levee, Arkansas

46. General description. Jacksonport Levee is a well sodded clay levee located near Jacksonport, Arkansas, approximately 15 ft high.

47. Overtopping data. Date - December 1982; maximum depth - 1 to 2 ft; duration - ± 1 week.

48. Damage. The levee was overtopped for 200 to 300 ft and breached where a roadway passed over the levee.

B. Everett Jordan cofferdam

49. General description. Formerly known as New Hope Dam, B. Everett Jordan Dam is an earth and rock fill dam approximately 115 ft high located near Moncure, North Carolina. During its construction, a permanent cofferdam,

approximately 30 ft high, consisting of intensely weathered rock (silty-clayey soil) was built. Upstream slopes were 1V on 2.5H with downstream slopes of 1V on 2H. The cofferdam was overtopped several times during the winter and spring of 1972-1973.

50. Overtopping data. Date - 3 February 1973; maximum height - ± 1 ft; duration - less than 24 hr.

51. Damage. Figure 16c, a general view of the construction site during overtopping, shows the partially complete inlet works and cofferdam. The cofferdam suffered a general erosion of the downstream slope with a sharp drop of the crest (Figures 16a and 16b). Because it served as a roadway, the upper center part of the crest was probably better compacted than the near surface soil on the downstream slope. Relief was provided by a crude spillway quickly cut in the left abutment seen at the right edge of Figures 16a and 16b and just at the left end of the cofferdam in Figure 16c.

McCarty Dam, Texas

52. General description. Owned and operated by the city of Albany, Texas, McCarty Dam was a sandy clay, rolled earth fill approximately 54 ft high and 1000 ft long. Located on Salt Prong Hubbard Creek, the dam had a 200-ft-wide uncontrolled spillway in the left abutment. The left end of the embankment, which formed the right spillway bank, was protected by grouted rubble. Upstream slopes were 1V on 3H for the lower portion and 1V on 2H on the upper portion, while the downstream slope was 2H on 1V.

53. Overtopping data. Date - 4 August 1978; maximum depth - unknown; duration - "long time" (apparently at least a few hours but less than 24 hr).

54. Damage. Figure 17 depicts general embankment damage. Though hydraulic conditions were not recorded, McCarty Dam provides an example of a breached and partially breached compacted earth fill of substantial size.

55. Apparently most, if not all, of the embankment was overtopped with breaching to the foundation occurring at the right abutment which was slightly lower than the rest of the embankment. The flow of water through the spillway probably produced a slope in the reservoir water surface from left to right (spillway to right abutment) along the crest, causing the greatest overtopping depth to occur at the right abutment. There is also some circumstantial evidence that seepage through the right limestone abutment may have aided breaching. Figures 18a and 18b are downstream views of embankment damage and reveal the chunkiness of embankment soil removal.

a. View from right abutment

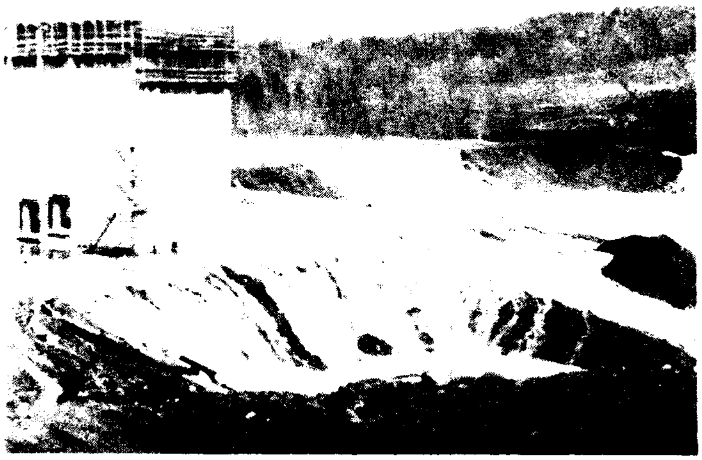

b. Overtopping damage

c. General view of overtopping

Figure 16. B. Everett Jordan cofferdam

Figure 17. General view showing overtopping damage to McCarty Dam

a. Slope erosion

b. Looking upstream into break at sta 7+57

Figure 18. Damage to downstream slope of McCarty Dam

Hart Hydro Dam

56. General description. Hart Dam is owned by the city of Hart in Oceana County in western Michigan and was used for power generation and recreation. The structure was an earthen embankment dam and included a concrete spillway and a 320-kw powerhouse. The dam is located on the South Branch of the Pentwater River. The CE inventory lists the structural height of the dam and head at 30 ft and a storage capacity of 4000 acre-ft. The impoundment size was 240 acres. The dam was about 600 ft long and was constructed of a clayey silty sand in 1927.* This embankment was constructed without an emergency spillway; however, the structure included two vertical gate-controlled spillways on either side of the powerhouse.

57. Overtopping data. This structure failed on 11 September 1986 after extensive efforts to save the dam including sandbagging and routing water over natural ground at the dam's west (left) abutment. Flow was forced over the left abutment by deliberately trenching with a backhoe. However, water eventually eroded from the point where the trench was discharging, near the embankment toe, up through the embankment with a resulting breach 200 ft wide and 35 ft deep. According to witnesses the initial breach (trench) was about 50 ft wide and 4 ft deep and was well controlled for about 4 hr (from 11:00 am to 3:00 pm on 11 September 1986) at which time a cascade-like waterfall developed on the downstream face of the embankment and large chunks of material began to break off and wash away. The mouth of the breach widened from 50 to 200 ft in about 45 min then began to deepen. The deepening process was slow and did not fully develop until more than 8 hr after the development of the waterfall. Observers state that the material at the downstream toe may have been sandy and easily erodible, allowing erosion to progress up into and finally through the center of the dam. The continuously increasing erosion level at Hart Dam was caused by unusually heavy rainfall and flooding over Michigan on 10 and 11 September 1986. As a result of the rainfall, it is estimated that the flood at Hart Dam peaked at 4000 cfs on 11 September with 2400 cfs passing through the spillway and powerhouse and 1600 cfs through the breach (Cook 1986). As the trench was first cut, there was no tailwater, but

---

* The embankment had a section about 25 ft across the crest with about a 1V on 3H slope on the upstream face and a 1V on 2H slope on the downstream face.

as the breach progressed and the reservoir emptied a tailwater built up to a height estimated to be 15 ft.

58. Damage. The breach resulting from the 11 September flood was 200 ft long and 35 ft deep. Hart city officials estimate the damage to be about $1,000,000 but say it might have been over $3,000,000 if the powerhouse and intake structure had been lost. The deliberate controlled breach was, in fact, attempted to protect the powerhouse and the initial trench was cut the maximum possible distance from the powerhouse.

Rainbow Lake Dam

59. General description. Rainbow Lake Dam is owned by a property owner association and is located on Pine Creek in Gratiot County in central Michigan. The structure was an earthen dam built in 1961 and was used primarily for recreation and impounds a reservoir of about 5400 acre-ft. The structure had no emergency spillway but did contain a rectangular drop inlet spillway. The CE inventory lists the structural height of the dam at 46 ft and the head at 42 ft. The dam is about 800 ft long, is 30 ft across the crest, and has upstream and downstream slopes of about 1V on 4H. The construction material was a well compacted sandy silty clay containing a small amount of very coarse gravel.

60. Overtopping data. As a result of extraordinarily heavy rainfall and flooding, this structure was overtopped and failed at about 2:00 am on Friday, 12 September 1986, after being overtopped for some 14 hr. The water level behind the dam had receded almost 6 in. when the embankment failed; however, the water over the crest reached a depth of from 18 to 24 in. An interviewed eyewitness stated, "Firemen walking across, wearing 18-in. boots got water in their boots." The eyewitness stated that erosion which resulted in the breach and failure of the embankment started in an area where vegetation cover was sparse or nonexistent due to the presence of a road or trail angling down the downstream side of the embankment. In years past the road had been used as a timber haul road and had been rutted in recent times by four-wheel-drive and all-terrain vehicles. Water, flowing down the embankment, channeled into the ruts of the road and about a half hour after overtopping began, erosion started about halfway down the embankment. The erosion then progressed up the roadway and through the embankment, breaching the structure in about 5 hr. No appreciable tailwater developed until the reservoir was almost completely released. The dam was overtopped by about 1.5 ft

of water and the peak discharge was estimated to be between 5000 and 6000 cfs. It is estimated that during peak discharge, the spillway was passing some 3000 cfs with the remainder passing over the dam (Cook 1986).

61. Damage. The breach resulting from the 12 September flood was about 100 ft wide and 35 ft deep. The entire reservoir was lost. Additional extensive damage resulted from water cascading down a second roadway which angled along the downstream face. The erosion mechanism could be observed in an arrested state because erosion had not progressed all the way through the embankment. The mechanism evidently consisted of the development of a characteristic water drop or cascade, as described by several observers, which caused progressive erosion at the toe aggravated by undercutting, sloughing, sliding, and removal of embankment material.

Summary

62. Documented cases of overtopped dams described above are summarized in Table 1. The data presented are necessarily sketchy and incomplete but these data and the description of events in the text generally suggest that homogeneous (monolithic) clay embankments tend to have greater resistance to breaching as a result of overtopping than do composite structures and those constructed of less plastic material. Complex, incomplete structures consisting of zones of dissimilar materials such as compacted clay against granular drains appear to be susceptible to damage possibly because of a lack of protection which would be provided in the complete structure, and because abrupt material discontinuities in incomplete structures may tend to erode under flowing water leaving rougher surfaces which produce turbulence and accelerate the erosion process.

Table 1

Overtopping Events

Embankment				Overtopping		Did pre-breach tailwater exist?	Did breach occur?
Name		Approximate Height, ft	Material	Max Depth, ft	Duration, hr		
R. D. Bailey cofferdam		60	Well graded sand and sandstone	6.5	4.0*	Y	Y
Bloomington cofferdam		30	Clayey sand gravel	5.0	10.0*	?	Y
Clarence Cannon cofferdam		45	Clay	5.0	20.0*	Y	Y
B. Everett Jordan cofferdam		30	Silt-clay	1.0	>24.0	N	N
Little Blue River levees		15	Clay (vegetated)	1.0	12.0**	N	N
Jacksonport levee		15	Clay	1-2	Approximately 1 week	?	Y
Elm Fork Structure 9		35	Clay (vegetated)	0.4	3.0	N	N
Colorado flood-retarding structures	M-1	38	SC-CL (vegetated)	1.0	2-4	N	N
	S-1	25		0.75	2-4	N	N
	W-1	47		2.5	1-2	N	N

(Continued)

* Elapsed overtopping time until breaching.
** During 1977 overtopping, no breaching; during 1982 overtopping, breaching after 20 hr.

Table 1 (Concluded)

Embankment			Overtopping		Did pre-breach tailwater exist?	Did breach occur?
Name	Approximate Height, ft	Material	Max Depth, ft	Duration, hr		
Upper Elk River and Big Caney watershed embankments	39-45	Clay and gravel	0.3-2.5	Unknown	?	N
Oros Dam	100	Zoned earth and rock fill	2.7	12-18*	--	Y
Armando de Salles Oliveira Dam	110	Earth fill	4.0	0.3*	--	Y
Euclides de Cumba Dam	200	Earth fill	4.0	7.5*	?	Y
McCarty Dam	54	Sandy clay	Unknown	"Few" <24.0	?	Y
Hart Hydro Dam	39	Clayey silty sand	1.0†	4.0*	N	Y
Rainbow Lake Dam	46	Sandy silty clay	1.5-2.0	14.0*	N	Y

* Elapsed overtopping time until breaching.
† Deliberate breach in effort to minimize damage.

PART III: BREACHING CHARACTERISTICS

Breaching Characteristics Reported by MacDonald and Langridge-Monopolis

63. MacDonald and Langridge-Monopolis (1984) compiled a list of 42 dams which failed. The list summarized pertinent information on size, geometry, reservoir characteristic, soil description, and cause of failure as well as breach characteristics. Not all of the structures which failed by breaching did so as a result of overtopping, but a significant number (15 out of 42) were overtopped. Summary tables by MacDonald and Langridge-Monopolis are shown here as Tables 2 and 3. The tables showed for a variety of dams, including some composite earth and concrete dams and earth and masonry dams as well as earth and rock fill zoned dams, that the most common terminal breach slope was 2V on 1H. The size of the breach is given in Figure 19 as the volume of material removed versus a breaching formation factor (BFF) which is defined as the product of the outflow of the total volume of water lost and the difference in elevation between the peak reservoir water surface and the breach base ($V_w \times h$). The data are presented on a log-log plot. Because the volume of water discharged is involved in the definition of BFF, the size of the reservoir is taken into account.

64. When all the points for which data are available in Figure 19 (31 points) are correlated using a log-log least squares fit, the coefficient of determination is 0.7227 which means that only about 28 percent of the total variation observed is unexplained by the correlation. Unexplained variation may be due to random fluctuations or to additional variables which have not been considered and taken into proper account. When the points in Figure 19 associated with overtopping only are analyzed (10 points) the coefficient of correlation becomes 0.7425.

65. Figure 20 is a log-log plot of breach development time versus volume of embankment material removed during breach given by MacDonald and Langridge-Monopolis (1984). A log-log least squares correlation of all the data in this figure (25 points) results in a coefficient of determination of 0.0385; if the data associated with overtopping only are analyzed (11 points), the coefficient of determination is 0.0014. These analyses suggest that no definitive correlation exists between breach development time and volume of

Table 2

Reported Characteristics of Dams Included in Study by MacDonald and Langridge-Monopolis (1984)

Dam Name	Dam No.	Date Constructed	Date Failed	Dam Height ft	Crest Width ft	Embankment Slopes Vertical:Horizontal Upstream	Embankment Slopes Vertical:Horizontal Downstream	Reservoir Storage Capacity acre-ft	Surface Area of Reservoir acres	Embankment Material	Cause of Failure
Apishapa	1	1920	1933	112	16	1:3	1:2	18,500	640	Fine sand	Piping
Baldwin Hills	2	1951	1963	160	63	1:2	1:1.8	897	19	Earth fill	Seepage
Buffalo Creek	3	1972	1972	46	420	1:1.6	1:1.3	392	13	Coal waste	Seepage
Bullock Draw Dike	4	1971	1971	19	14	1:2	1:3	918	—	Earth fill	Piping
Castlewood	5	1890	1933	70	16	1:3	1:1	3,430	200	Rock with masonry wall	Overtopping
Cheaha Creek	6	1970	1970	23	14	1:3	1:2.5	56	—	Zoned earth fill	Overtopping
Davis Reservoir	7	1914	1914	39	20	1:2	1:2	47,000	3,200	Earth with concrete facing	Piping
Euclides da Cunha (Brazil)	8	1958	1977	174	—	—	—	11,000	—	Earth fill	Overtopping
Frankfurt (Germany)	9	1975	1977	32	—	—	—	285	—	Earth fill	Seepage
French Landing	10	1925	1925	40	8	1:2	1:2.5	—	—	Earth fill	Seepage
Frenchman Creek	11	1952	1952	41	20	1:3	1:2	17,000	—	Earth fill	Piping
Goose Creek	12	1903	1916	20	10	1:1.5	1:1.5	8,590	—	Earth fill	Overtopping
Hatchtown	13	1908	1914	63	20	1:2	1:2.5	12,000	—	Earth fill	Seepage
Hebron	14	1913	1914	38	12	1:3	1:1.5	—	—	Earth fill	Piping
Hell Hole	15	1964	1964	220	70	1:1.5	1:1.5	—	—	Rock fill	Overtopping
Horse Creek	16	1911	1914	40	16	1:1.5	1:2	17,000	1,200	Earth with concrete facing	Seepage
Johnston City	17	1921	1981	14	6	1:4.75	1:2.75	466	—	Earth fill	Seepage
Johnstown (South Fork Dam)	18	1853	1889	75	10	1:2	1:1.5	15,340	407	Earth and gravel fill	Overtopping
Kelly Barnes	19	1948	1977	38	20	1:1	1:1	410	42	Earth fill	Piping
Lake Frances	20	1899	1899	50	16	1:3	1:2	700	43	Earth fill	Piping
Laurel Run	21	—	1977	42	—	—	—	307	—	Earth fill	Overtopping
Little Deer Creek	22	1962	1963	86	—	—	—	1,400	—	Earth fill	Piping
Lower Otay	23	1897	1916	135	12	1:1	1:1	—	—	Rock fill	Overtopping
Lower Two Medicine	24	1913	1964	37	—	—	—	16,000	—	Earth fill	Overtopping
Lyman	25	1913	1915	65	12	1:2	1:2	40,000	—	Earth with clay core	Seepage
Lynde Brook	26	1870	1876	41	50	1:2	1:2.3	2,040	132	Earth with core wall	Seepage
Melville	27	1907	1909	36	10	1:3	1:1.5	—	—	Earth with core wall	Seepage
North Branch Tributary	28	—	1977	—	—	—	—	—	—	Earth fill	—
Oros	29	1960	1960	116	—	—	—	527,000	—	Earth fill	Overtopping
Otto Run	30	—	1977	—	—	—	—	—	—	Earth fill	—
Rito Manzanares	31	—	1975	24	12	1:1.34	1:1.34	20	—	Earth fill	Seepage

(Continued)

Table 2 (Concluded)

Dam Name	Dam No.	Date Constructed	Date Failed	Dam Height ft	Crest Width ft	Embankment Slopes Vertical:Horizontal Upstream	Embankment Slopes Vertical:Horizontal Downstream	Reservoir Storage Capacity acre-ft	Surface Area of Reservoir acres	Embankment Material	Cause of Failure
Salles Oliveira	32	1966	1977	115	—	—	—	21,000	—	Earth fill	Overtopping
Sandy Run	33	—	1977	28	—	—	—	46	—	Earth fill	Overtopping
Schaeffer	34	—	1921	100	15	1:3	1:2	3,190	—	Earth with concrete core	Overtopping
Sheep Creek	35	1969	1970	56	20	1:3	1:2	1,160	85	Earth fill	Seepage
Sinker Creek	36	1910	1943	70	—	—	—	2,700	—	Earth fill	Seepage
South Fork Tributary	37	—	1977	—	—	—	—	—	—	Earth fill	—
Spring Lake	38	1887	1889	18	8	1:0.75	1:0.75	110	18	Clay and gravel	Piping
Swift	39	1914	1964	189	—	—	—	30,000	—	Rock with concrete facing	Overtopping
Teton	40	1972	1976	305	35	1:3	1:2.5	288,250	—	Zoned earth fill	Piping
Wheatland No. 1	41	1893	1969	45	20	—	—	—	—	Earth fill	Piping
Winston	42	1904	1912	24	7	1:1		—	—	Earth with rubble core	Overtopping

Table 3

Flow and Breach Characteristics

Dam Name	Dam No.	Outflow Volume V_w, ft acre-ft	Difference in Elevations[b] h, ft	Breach Formation Factor $V_w \times h$ acre-ft x ft	Peak Rate of Outflow, Q cu ft/sec	Crest	Shape	Top Width ft	Depth ft	Side Slope Vertical:Horizontal	Material Removed cu yd	Maximum Development Time, hr
Apishapa	1	18,000	91.0	1,638,000	242,000	600	Trapezoid	320	100	6:7:1 and 2.9:1	291,000[c]	2.5
Baldwin Hills	2	738	60.0	44,300	34-40,000	650	Triangular	75	90	2.4:1 and 2.4:1	29,000[c]	1.3
Buffalo Creek	3	392	46.0	18,000	50,000		Trapezoid	435	46	0.5:1 and 0.5:1	417,000	0.5
Bullock Draw Dike	4	600	10.0	6,000	--		Trapezoid	45	19	4.75:1 and 4.75:1	1,700[c]	—
Castlewood	5	7,500	71.0	532,500	126,000		Trapezoid	180	70	--	72,800[c]	0.33
Cheaha Creek	6	--	--	--	--		--	--	--	--	20,300	5 to 6[f]
Davis Reservoir	7	--	38.0	—	18,000		Trapezoid	70	39	Vertical and 2:1[a]	8,460[c]	7.0
Euclides da Cunha (Brazil)	8	47,000[3]	191 0	9,000,000	--		Trapezoid	—	174[a]	--	949,000[c]	7.3
Frankfurt	9	285	27.0	7,700	--	1,000	Trapezoid	31	32[a]	2.5:1 and 2.5:1	1,690[c]	0.25[a]
French Landing	10	3,140[3]	28.0	87,920	32,800		Trapezoid	135	46.5	--	18,000	0.58
Frenchman Creek	11	13,000	35.5	461,500	50,000		Trapezoid	220	41	2:1 and 2:1[a]	37,100[c]	—
Goose Creek	12	470[3]	4.5	2,120	20,000		Trapezoid	100	13.5	2:1 and 2:1[a]	1,400[c]	0.5
Hatchtown	13	13,600	52.0	707,200	110-247,000		Trapezoid	590	65	1:1 and 1:1	210,000[c]	3.0
Hebron	14	--	40.0	—	--		Trapezoid	200	50	2:1 and 2:1[a]	40,300[c]	1 to 3.5
Hell Hole	15	24,800	100.0	2,480,000	260,000		Trapezoid	—	220[a]	--	726,000[c]	5.0
Horse Creek	16	6,000	27.0	162,000	--		Trapezoid	250	40	1:1 and 1:1	26,800[c]	—
Johnston City	17	466	10.0	4,660	--		Trapezoid	44	17	1:1 and 1:1	800[c]	—
Johnstown (South Fork Dam)	18	15,340	73.0	1,119,820	200-300,000		Trapezoid	420	50-200	--	90,000	3.5
Kelly Barnes	19	630	34.0	21,420	24,000		Trapezoid	115	38	1:1 and 1:0.5	13,000	--
Lake Frances	20	640	40.0	25,600	--		Trapezoid	98	50	1:6:1 and 1.6:1	16,200	1.0
Laurel Run	21	310	42.0	13,020	37,000		--	--	--	--	--	--
Little Deer Creek	22	1,000	55.0	55,000	47,000		Trapezoid	75	70	--	--	0.33
Lower Otay	23	--	--	—	--		Trapezoid	—	135[a]	--	140,000	0.33
Lower Two Medicine	24	20,930	36.0	753,500	63,500		Trapezoid	--	--	--	--	—
Lyman	25	29,000	53.0	1,540,000	--		Trapezoid	350	65	2:1 and 1:1	94,000	—
Lynde Brook	26	2,330	40.0	93,200	--		Trapezoid	150	40	1:1.3 and 1:1.3	20,000[c]	3.0
Melville	27	20-30,000	30.0	750,000	--		Trapezoid	130	36	1:3.6 and 1:3.6	13,890	—
North Branch Tributary	28	18	18.0	324	1,040		--	--	--	--	--	—
Oros	29	527,000	116.0	61,132,000	340-480,000		Trapezoid	660	116	--	1,000,000	—
Otto Run	30	6	19.0	114	2,120		--	--	--		--	—
Rito Manzanares	31	20	15.0	300	--		Trapezoid	62	24	1.3:1 and 1.3:1	1,690[c]	—

(Continued)

Table 3 (Concluded)

Dam Name	Dam No.	Outflow Volume V_w, ft acre-ft	Difference in Elevations[b] h, ft	Breach Formation Factor V_w x h acre-ft x ft	Peak Rate of Outflow, Q cu ft/sec	Crest	Shape	Top Width ft	Depth ft	Side Slope Vertical:Horizontal	Material Removed cu yd	Maximum Development Time, hr
Salles Oliveira	32	58,000[3]	126.0	7,310,000	--		Trapezoid	--	115[a]	--	576,000[c]	2.0
Sandy Run	33	46	28.0	1,288	15,300		--	--	--	--	--	--
Schaeffer	34	3,600	90.0	32,400	153-174,000		Trapezoid	690	90	--	296,900[c]	0.5
Sheep Creek	35	2,360[3]	46.0	108,600	--		Trapezoid	100	56	2:1 and 2:1	23,900	--
Sinker Creek	36	2,700[4]	70.0	189,000	--		Trapezoid	300	70	2:1 and 2:1[a]	110,000[c]	2.0
South Fork Tributary	37	3	6.0	18	4,300		--	--	--	--	--	--
Spring Lake	38	110	18.0	1,980	--		Trapezoid	65	18	2:1 and 2:1[a]	800[c]	--
Swift	39	30,000	157.0	4,710,000	881,000		Trapezoid	--	189[a]	--	270,000	0.25[a]
Teton	40	251,000	220.0	55,200,000	1,300,000		Trapezoid	--	220	--	4,000,000	6.0
Wheatland No. 1	41	9,400	40.0	376,000	--		Trapezoid	150	45	2:1 and 2:1[a]	19,100[c]	1.5
Winston	42	537	25.0	13,400	--		Trapezoid	70	24	5:1 and 5:1	1,940[c]	5.0

Note: 1 acre-ft = 1,233 m^3; 1 ft = 0.305 m; 1 cfs = 0.0283 m^3/s; 1 yd^3 = 0.765 m^3. (From McDonald and Landridge-Monopolis 1984)

[a]Assumed values.

[b]Initial water surface elevation minus base elevation of breach.

[c]Calculated values.

[1]Highly resistant core material.

[2]Breach restricted by concrete structure.

[3]Outflow volume very approximate.

[4]Reservoir full at time of failure.

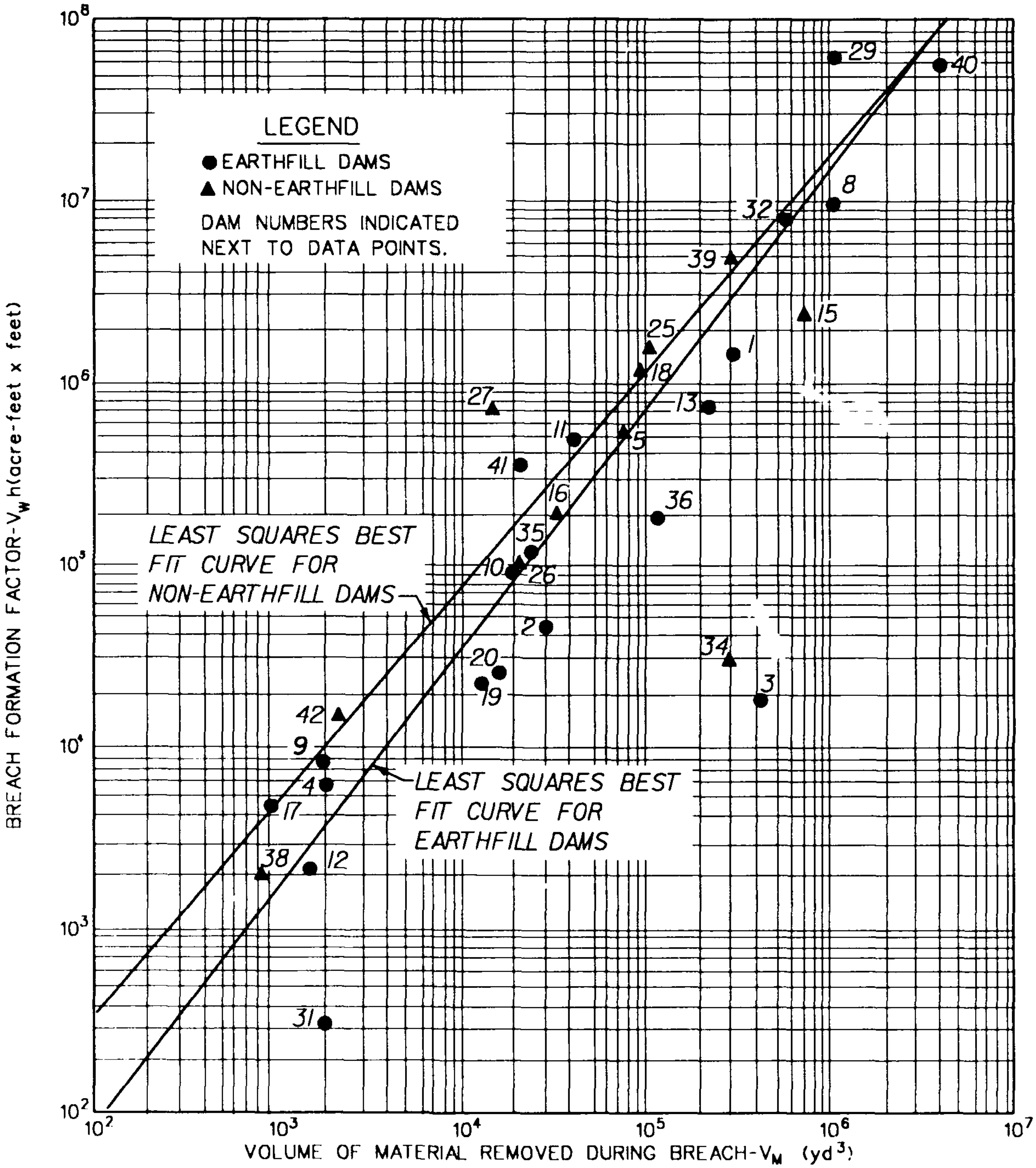

Figure 19. Outflow characteristics versus breach size (MacDonald and Langridge-Monopolis 1984)

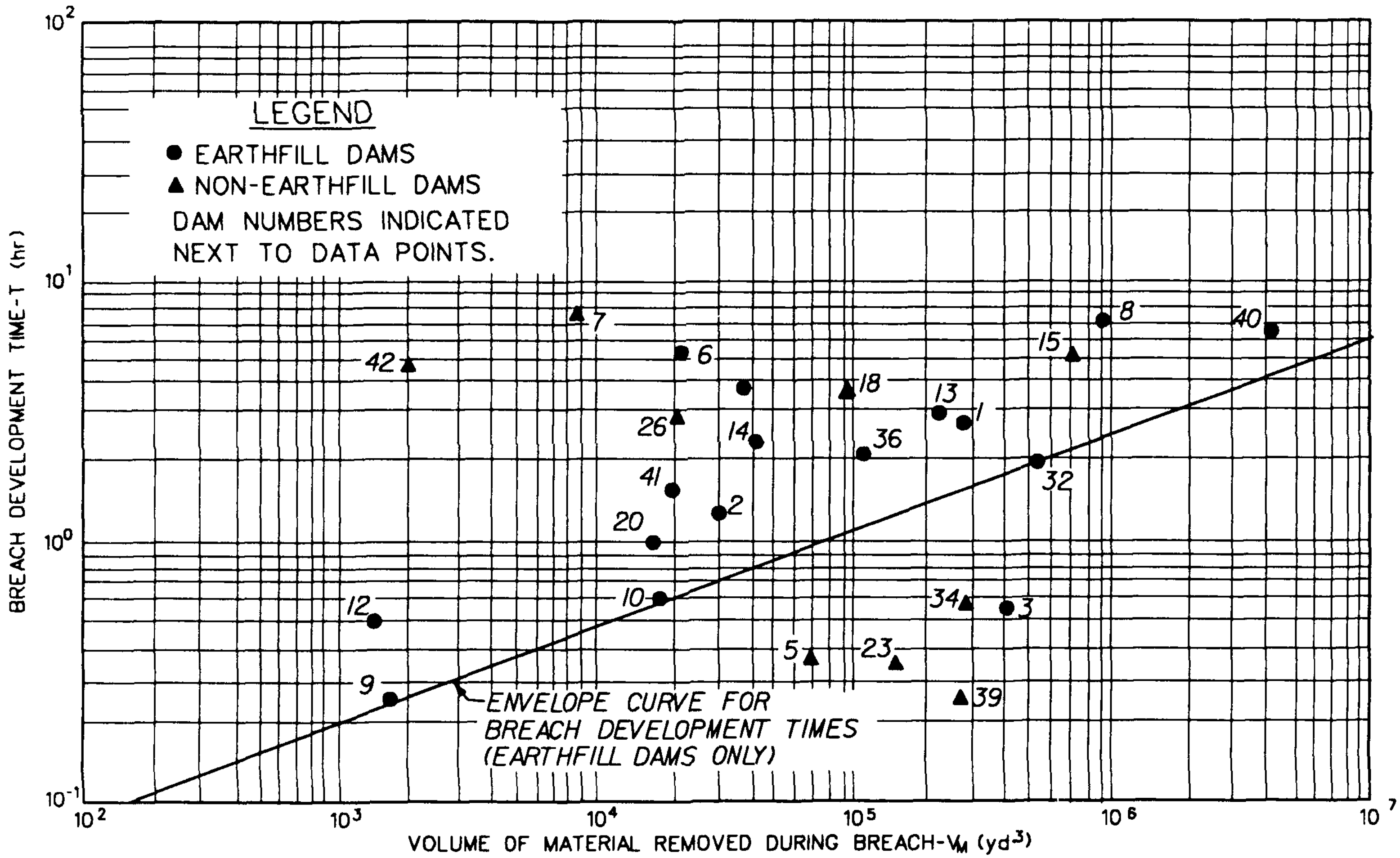

Figure 20. Breach size versus breach development time (MacDonald and Langridge-Monopolis 1984)

material removed. MacDonald and Langridge-Monopolis suggest that composite dams (which consist of earth and concrete or other non-earth internal elements) are subject to sudden collapse (short breach development time) because of structural instability. This may be observed in model and prototype behavior, but these data designed to illustrate the point fail to correlate convincingly. There are, undoubtably, other significant variables involved in the process between time and amount of material removed which the authors have failed to identify and include in their analyses. From these analyses, it may be concluded that the processes involved in overtopping and breaching of dams are complex and the data to explain and correlate the variables may be incomplete or unavailable.

66. Figure 21 shows the relationship between breach formation factor and peak rate of outflow from the breach. If all the data are considered in a least squares fit, the coefficient of determination is 0.8408; if the overtopping data only are considered the coefficient is 0.7352. The correlation of the variables in Figure 21 is thought to be reasonably good considering that an important variable which is not taken into account in this analysis is geometry and topology of the associated reservoir.

67. Data from the correlations by MacDonald and Langridge-Monopolis are presented here because they represent actual field behavior of full-size dams. The authors qualify their results stating that the relationships developed are those for normal materials and geometries and may be inappropriate for highly erodible dams or dams that are subject to liquefaction as well as dams having extremely wide or narrow embankments or embankments with other unique features which influence breaching characteristics.

Overtopped Dams Reported by Ponce

68. In a literature survey by V. M. Ponce (1982), cases of earth dam breaches dating from about the turn of the century to the late 1970's are summarized. Ponce used this information to confirm a Corps of Engineers (USAWES 1961) dam breach correlation which relates a Froude number based on peak discharge during a breaching event to a shape factor which is defined in terms of breach dimensions, embankment size, and geometry. The 1961 work at the Waterways Experiment Station (WES) was based on flume studies in which models of specified geometric cross section and roughness characteristics were tested.

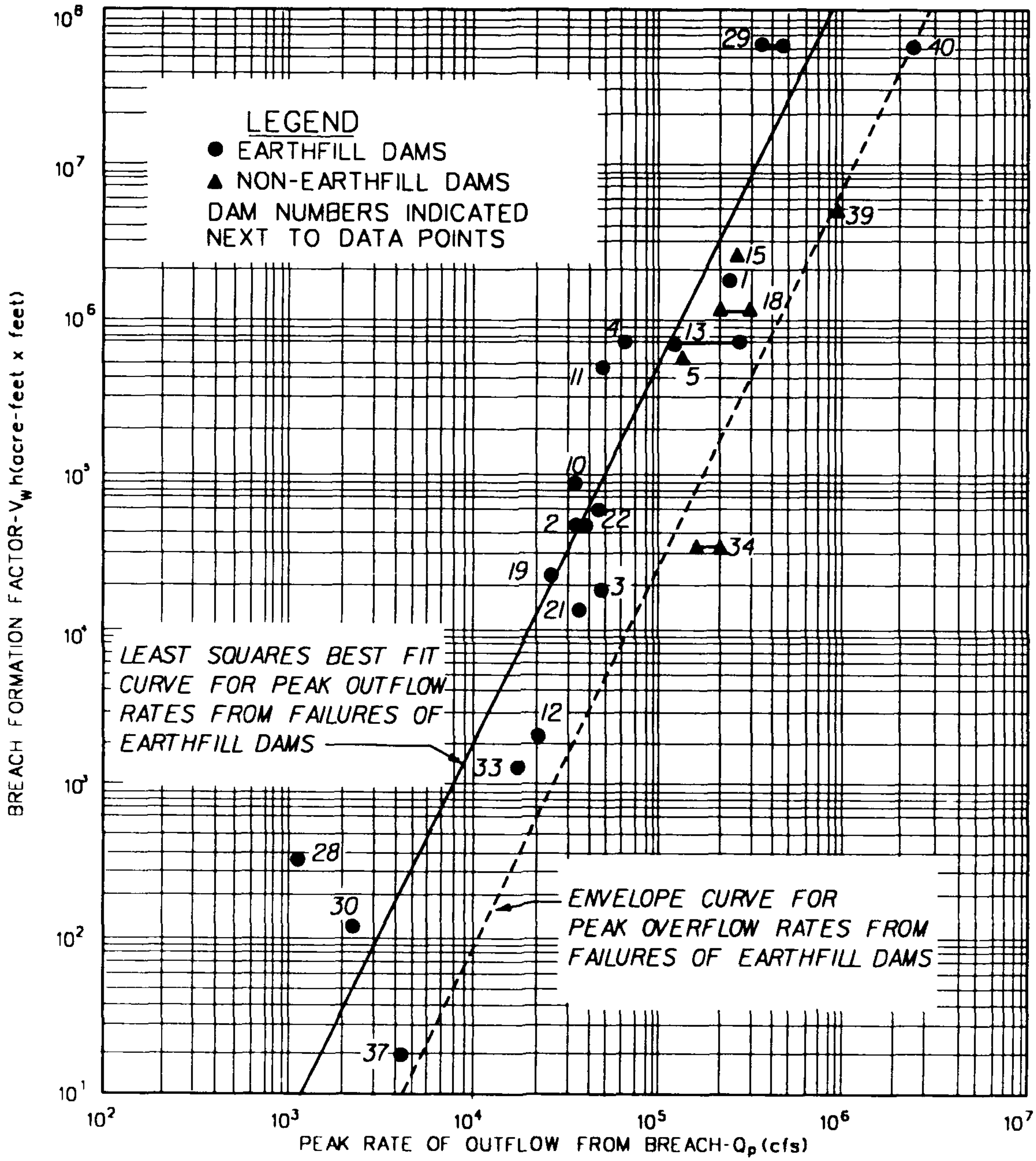

Figure 21. Outflow characteristics versus peak rate of outflow (MacDonald and Langridge-Monopolis 1984)

Failures were simulated by an almost instantaneous removal of part or all of the embankment. Therefore the WES study would be representative of sudden failure but not gradual failure and it must be noted that the hydraulics of the two cases are very different. The Froude number F and shape factor S utilized in the study are defined as

$$F = \frac{Q_p}{W_b(gD_b^3)^{1/2}} \tag{1}$$

and

$$S = \frac{W_b D_b}{W_d Y_o} \tag{2}$$

where

Q_p = peak discharge, ft^3/sec

W_b = top width of breach, ft

g = acceleration due to gravity, 32.2 ft/sec^2

D_b = average depth of breach, ft

W_d = top width of dam, ft

Y_o = maximum depth of dam, ft

The correlation determined from the WES study was

$$F = 0.29\ S^{-0.28} \tag{3}$$

which can be compared to

$$F = 0.20\ S^{-0.39} \tag{4}$$

determined by Ponce (1982) and stated to be "an equation encompassing the upper limit of the data." But this equation clearly is not the upper limit of the data in that eight points are shown above the envelope defined by the equation. If a least squares log-log linear fit is performed to correlate

Froude number F and shape factor S for the 25 cases reported by Ponce for which adequate data are available to determine F and S , the coefficient of determination is 0.1738, and if the data involving embankment breach and failure by overtopping only is considered, the coefficient is 0.0413.

69. The low correlation coefficients point to the fact that correlation between these variables is weak if it exists at all, and that there are significant factors which have not been taken into account by Ponce. However, it must be realized that data are often sketchy in historically reconstructed case studies.

70. The equation determined by a least square fit of the 1982 data by Ponce is

$$F = 0.10\ S^{-0.41} \tag{5}$$

71. Many of the cases of prototype failure reported by Ponce involved breaching as a direct result of overtopping and those have been listed in Table 4 along with two overtopped Michigan dams researched during this investigation. Cases of dam breaches from causes other than overtopping reported by Ponce are summarized here in Table 5. In many cases, details from the historical literature were sketchy and certain values pertinent to Ponce's investigation had to be extrapolated or estimated, but two fairly significant conclusions may be drawn from these data.

72. First, the overtopping failures reported by Ponce in all cases except one occurred as the result of unusually heavy precipitation, and represented about half of the failures reported from causes which could be identified. These data suggest that a substantial number of embankment failures are preventable by providing an appropriate combination of adequate spillway capacity and emergency flood diversion facilities so as to prevent overtopping.

73. The second suggestion of these data may be significant for modeling and designing models to study overtopped dams. The data reported in the tables spanned structures ranging from small, old, unengineered dams with probably little construction control, to large, modern, well engineered and controlled structures. A significant problem in the analysis or modeling of any structure of this type is the selection and justification of dimensional

Table 4

Summary of Overtopped Dams Taken from Literature

Embankment	Year Built/Failed	Height ft	Reservoir Capacity acre-ft	Peak Discharge ft^3/sec	Breach Width ft	Breach Depth ft	Time of Failure hr	Cause of Overtopping Failure	Crest Width ft	Breach Width/ Crest Width
Break Neck Run Dam (Pennsylvania)	1877/1902	23	40	325*	100	23*	3.0*	Cloudburst	207	0.48
Sherburne Dam (New York)	1883/1905	34	61	500*	150	34*	3.0*	Severe rainstorm	300	0.50
Dells Dam (Wisconsin)	1910/1911	59	10,580	191,940*	370	59	0.67*	Heavy rainfall	960	0.39
Hatfield Dam (Wisconsin)	1908/1911	22	9,923	120,000*	300	22*	2.0*	Heavy rainfall upstream reservoir release	450	0.67
Goose Creek Dam (South Carolina)	1903/1916	20	8,600	17,400*	100	13	12.0*	Heavy rainfall	2,300	0.04
Puddington Dam (California)	----/1926	50*	500	10,000	300	35*	3.0*	Clogged flood-diversion channel	825	0.36
Hemet Dam (California)	1923/1927	20	7,000	56,500*	100*	20	3.0*	Heavy rainfall	273	0.37
Elk City Dam (Oklahoma)	1925/1936	30	600	21,500	150	30	0.83*	Cloudburst	850	0.18
Frenchman Dam (Montana)	1951/1952	40	7,010	56,600*	800*	40*	3.9*	—	2,900	0.28
Knife Lake Dam (Minnesota)	----/1972	20	8,000	38,800*	40*	20*	5.0*	Torrential rains	200	0.20
Rainbow Lake (Michigan)	1961/1986	46	5,400	5-6,000*	100	35	14.0	Severe rainstorm	800	0.13
Hart Hydro Dam (Michigan)	1927/1986	39	4,000	4,000*	200	35	8.0	Severe rainstorm	600	0.33
Euclides da Cunha (Brazil)	1958/1977	174*	11,000	35,500	430	174	7.25	Severe rainstorm	1,000	0.43
Armando de Salles Oliveira Dam (Brazil)	1966/1977	115*	21,000	254,100*	550	115	2.0	Severe rainstorm	2,165	0.25

* Estimated.

Table 5

Summary of Breached Dams from Various Causes Taken from Literature

Embankment	Year Built/Failed	Height ft	Reservoir Capacity acre-ft	Discharge ft^3/sec	Breach Width ft	Breach Depth ft	Time of Failure hr	Cause of Failure	Crest Width ft	Breach Width/ Crest Width
Lake Avalon (New Mexico)	1894/1904	48	6,300	82,000	450*	48*	2.0*	Leakage/burrowing animals	1,380	0.33
Horse Creek Dam (Colorado)	1911/1914	55	17,000	137,140	200	42	3.0*	Piping	600	0.33
Hatchtown (Utah)	1908/1914	65	12,000	60,600	120*	65*	4.0*	Seepage	780	0.15
Mammoth Dam (Colorado)	1916/1917	70	11,000	89,000*	30	70*	3.0*	Inadequate spillway	160	0.19
Balsams Dam (New Hampshire)	1927/1929	60	—	—	110	60*	—	Erosion from spillway	300	0.37
Sinker Creek Dam (Idaho)	1910/1943	70	2,700	—	300	70*	3.0*	Seepage	1,100	0.27
Baldwin Hills Reservoir Dam (California)	1951/1963	160	897	5,000*	400*	160*	4.5*	Subsidence	550	0.73
Lake Latonka (Pennsylvania)	1965/1966	43	1,290	10,400*	110*	43	3.0*	Embankment failure	2,300	0.05
Nanaksagar Dam (India)	1962/1967	52	170,000	342,900*	150	52*	12.0*	Leakage	10,560	0.01
Wheatland No. 1 (Wyoming)	1893/1969	45	9,370	151,200*	150	45*	1.5	Embankment failure	6,600	0.02
Whitewater Brook Upper Dam (New Hampshire)	1943/1972	62	420	2,500*	21	20	3.0*	Erosion of spillway	450	0.05
Teton Dam (Idaho)	——/1976	305	288,000	1,652,300	150	261	4.0*	Piping	3,100	0.05
Kelly Barnes Dam (Georgia)	1940/1977	26	400	19,400*	450	26*	0.5	Unknown	500	0.90
Frankfort Dam (West Germany)	1975/1977	32	285	2,800*	31	32*	2.5	Unknown	393	0.08

* Estimated.

representation. For the problem under consideration here, the question of dimensional representation becomes "Can an overtopped dam be adequately represented in two dimensions, or will three-dimensional representation be required?" Representation in three dimensions is obviously much more difficult than representation in two, but since the ultimate objective of any modeling technique is to be able to predict prototype behavior, it may serve well to study and learn lessons from prototype behavior.

74. In two-dimensional representation, the assumption generally made is that the effect of the third dimension is unimportant. No change occurs with, nor is there any influence of, the third dimensions. This means, generally, that two-dimensional representation will be adequate if what happens to one plane in two dimensions, happens to all planes. Table 4, which is a summary of dam breaches that occurred as the result of overtopping only, and Table 5, which summarizes dam breaches that occurred from a variety of causes, suggest that two-dimensional representation is not adequate. This may be demonstrated relatively simply by comparing the length of breach to the total embankment length. If an entire embankment or a significant portion of it is lost during a breach then all (planar) cross sections are behaving similarly, there is no variation in behavior along the length of the embankment, and two-dimensional representation is adequate. If, on the other hand, breach behavior is local, there is a significant influence of the third dimension, and two-dimensional representation of the structure may not be adequate unless a way can be found to estimate breach width beforehand.

75. The ratio of breach width to (total) crest width is shown in Table 4 for all the structures reported by Ponce (which were breached as the result of overtopping). If two-dimensional representation is adequate, this ratio should approach unity. Examination of these tables shows that this is not the case. Only in one case is this ratio greater than one-half. For all others, the values are one-half and substantially less than one-half in many instances. This means that embankment cross sections are not independent of position in the embankment, and that substantial differences in behavior may be found between models based on two-dimensional and three-dimensional representation. It is significant that this trend is seen in prototype data for a wide range of embankment types, sizes, geometric designs, and construction techniques.

PART IV: CENTRIFUGE MODELING

Background

76. The most direct and reliable of methods to obtain information on the performance of an overtopped dam and the resultant damage is to build the full-size embankment to be evaluated, instrument it, then induce hydrodynamic conditions which will cause overtopping and failure while acquiring data which could be related to the behavior of the entire system. This, of course, is the description of a full-scale prototype test and is unreasonable from the standpoint of prohibitive cost, time, inconvenience, and danger to life and property. Even if it were possible to test a particular prototype configuration to destruction, the exercise would be instructive of only the behavior of that specific embankment/reservoir/hydrodynamic load system.

77. It would be very convenient if small inexpensive scale models which would closely duplicate the behavior of full-size structures could be constructed and tested to destruction in the laboratory. Within reason, this may be possible by building and testing a properly designed and scaled physical model.

78. Physical modeling is a well known approach to solving engineering problems so complex that they are not amenable to exact mathematical solution. The problem of the overtopped dam under consideration here is one well suited for investigation by physical modeling since it is a problem which must be represented by three phases (solid, liquid, gas) and in three dimensions. The system consists of a solid with nonlinear material properties and complex boundary conditions. Since the solid structure is subjected to overtopping, a hydrodynamic process results which involves unsteady, nonlinear flow conditions; because the solid material is erodible the problem becomes one involving movable boundaries. An additional complicating factor is that the stress-strain and strength characteristics of the solid (which is generally soil) are stress and time dependent. At this writing, no analytical model exists which can take all these factors into account. Obviously, the state of stress in a small-scale model of a soil structure under normal self-weight (gravity) loading will be much different than the state of stress in a full-size prototype. Because of the stress-dependent constitutive behavior of soil, quantitative and even qualitative differences in behavior might be

expected between a small-scale model and the corresponding full-size prototype structure. This is to say that unless other measures are taken in the small-scale modeling of soil structures, not only will measurable parameters such as stress, deformation, and pressure in the model be different from those in the prototype, but observed failure mechanism may also be quite different in the model than in the prototype.

79. However, if a small-scale model of a soil structure could be placed in a field where acceleration could be increased so that stress level due to self-weight in the model could be matched with the corresponding stress level existing in the prototype, then many of the problems and limitations associated with testing a small-scale model of soil would be removed. Acceleration above normal gravity (1 g) can be achieved through the use of a centrifuge device. However, other requirements must be fulfilled for the design of a satisfactory model experiment. Similitude must exist between model and prototype to achieve equivalent behavior between these two systems.

Similitude

80. Similitude between model and prototype means that there must exist geometric and dynamic similarity between model and prototype (Dailey and Harleman 1973; Baker, Westine, and Dodge 1973). In a strict sense, geometric similarity means that the ratio of all corresponding lengths in the two systems must be the same. The basic concept of dynamic similarity is the requirement that the two systems in question with geometrically similar boundaries have geometrically similar flow patterns at corresponding instants of time. Therefore, all individual external and internal forces acting on corresponding elements of mass must have the same ratios in the two systems.

81. Strict fulfillment of these requirements is generally impossible except with a 1:1 scale ratio. Fortunately, it is often possible to group significant parameters in dimensionless ratios and match these dimensionless ratios between model and prototype to achieve equivalence between the two systems. There are two commonly used techniques to methodically group parameters into dimensionless ratios:

- a. Manipulation of the governing differential equations.
- b. An algebraic method known as the Buckingham PI theorem.

82. The Buckingham PI theorem (E. Buckingham 1915) provides a very straightforward method by which the physical quantities required to describe systems can be organized into the smallest number of significant dimensionless groups. The theorem proves that in a physical problem involving q quantities (such as velocity, pressure, stress, etc.) in which there are m fundamental dimensions (force, length, time, and temperature), the quantities may be arranged into (q-m) independent dimensionless parameters.

83. A natural consequence of the PI theorem is that if m fundamental dimensions are used within a system, then m assumptions must be made to determine the scaling relationship with a companion system. This means that there is no unique modeling system which will satisfy similitude. There are literally an infinity of models which will satisfy similitude. However, not all these models are practical and physically reasonable. A model must be chosen which is both feasible and which will allow the dimensionless ratios mentioned above to be matched closely enough that similar behavior occurs between prototype and model.

84. The fact that a modeling system which satisfies similitude is not unique means that model experiments may be designed at any scale or under any acceleration level which satisfies similitude. Using scaled geometric sizes with unscaled material particle sizes in a 1 g gravitational field often means sacrificing some similitude for the sake of modeling simplicity. This is often done in flume modeling studies which will be discussed later. It is difficult to achieve similitude in a 1-g field without the use of dissimilar model materials, the properties of which are discussed by Gilbert, Hale, and Kim (1985). The design of an appropriate dissimilar material with correct properties is very difficult. However, by increasing acceleration on the model, as in a centrifuge, prototype soil will often serve as the model material and will behave "correctly" in terms of stress-strain and strength characteristics. Unfortunately there are other difficulties related to centrifuge modeling involving time scaling which will cause problems in achieving similitude. They will be discussed later.

85. In centrifuge modeling, there is a direct scaling relationship between events in the model and events in the prototype and they can be derived from either the PI-theorem or by manipulation of the governing differential equation. Scott and Morgan (1977) compiled a list of such relations and they are shown on Table 6.

Table 6

Scaling Relations (Scott and Morgan 1977)

Quantity	Full Scale (Prototype)	Centrifuge Model at n, g
Linear dimension	1	1/n
Area	1	$1/n^2$
Volume	1	$1/n^3$
Time		
Dynamic events	1	1/n
Hydrodynamic events	1	$1/n^2$
Viscous flow	1	1
Velocity, distance/time	1	1
Acceleration, distance/time^2	1	n
Mass	1	$1/n^3$
Force	1	$1/n^2$
Energy	1	$1/n^3$
Stress, force/area	1	1
Strain, displacement/unit length	1	1
Density	1	1
Frequency	1	n

Difficulties and the Need for Further Research

86. There are a number of difficulties which will require further research and development for proper resolution. Some of the difficulties which may impact centrifuge modeling studies are:

a. There is a conflict in time scaling between model and prototype for certain events.

b. Particle size effects result from not scaling model material particle sizes.

c. As a result of a. and b., there are unresolved problems associated with the simulation of dynamic and hydrodynamic events.

Conflict in time scaling

87. As can be seen in Table 6, there is an anomaly in scaling of time among dynamic events governed by the wave equation (1/n), steady-state flow events governed by the diffusion equation ($1/n^2$), and viscoelastic events

(1/1) which do not model. Therefore, it is impossible to establish similarity between model and prototype when the above phenomena occur simultaneously in the prototype. However, there may be an alternate way to resolve the difficulty in similitude between hydrodynamic events and dynamic events, except for viscoelastic events. Dimensional analysis suggests that events involving conflicts in time scaling may be facilitated if the coefficient of permeability k is increased by a factor of n using viscous pore fluids (mixture of water and oil and/or glycerin). Whitman, Lambe, and Kutter (1981) and Lambe and Whitman (1982) have used viscous pore fluids to advantage in dynamic testing, yet more research is needed to confirm the validity of this approach in overcoming the time scaling conflict. The relations governing erosion are not sufficiently understood to establish a method of scaling time in dam breaching even at this stage.

Modeling particle size

88. In order to avoid many difficulties associated with satisfying similarity in scaling relations, experimenters generally use prototype soil and water in the model. Questions arise: Is the stress-strain-strength behavior the same in model material as in the prototype? Is erosion behavior similar? It is conceivable that model behavior may be different from the corresponding prototype behavior since linear dimensions of soil particles are not scaled in the same proportion as that of other features of the model. Detailed studies focused on investigation of these uncertainties have not been conducted in the past and are considered worthwhile because improperly scaled particle sizes could interact to produce problems in other areas. Some of these problems will be discussed below.

Simulation of Hydrodynamic Events

89. A prototype embankment which is overtopped is simultaneously subjected to seepage and accompanying seepage forces and pressures. Because prototype soil is usually used directly as model material, the particle and void sizes in the model are improperly scaled. Therefore any property which interacts with particle size and pore size, such as seepage discharge, will not model correctly. Additionally flow velocity through the voids will not model correctly, so similitude will not be achieved between model and prototype for seepage forces and pressures. This could be significant for

structures of sandy soils or structures containing sandy seams or zones, as disproportionately high seepage velocities could cause premature failure.

90. The problem of seepage will not be as significant in clay embankments where particle and void size would be less exaggerated between model and prototype. However, impermeable plastic clays are generally subject to creep deformation, which is viscous flow, and from Table 6 it is seen that viscous flow is independent of g-level, that is, it does not model. Therefore, after erosion begins propagating its way through the centrifuge model and sloughing and sliding begin as a result of embankment oversteepening, if the material rate of deformation is subject to time influences, then the rate of breach will not proceed correctly (as a function of time) in the model. Therefore, breach development and discharge history will be distorted in the model. Additionally, because particle sizes are not modeled correctly, sediment transport rate and therefore rate of erosion may not be properly modeled.

91. These sorts of uncertainties arise because different phenomena, all of which are significant to the problem under consideration, proceed at very different time scales. Simulation of collapse mechanism and prediction when collapse begins as the result of overtopping are the desired objects of a model study; if events which lead to collapse do not proceed correctly in time, then there is no assurance that collapse mechanism will be correct. For example, if a seepage "blow out" occurs prematurely as a result of incorrect particle size distribution, then breach size, shape, and rate of development will certainly be affected. Events must proceed similarly in time between model and prototype to ensure that collapse mechanism is faithfully reproduced. If centrifuge modeling is ever to answer the question "How long can overtopping occur before the structure fails?", additional research is needed in this area of centrifuge modeling to resolve these complex issues.

Centrifuge Model Studies by Ko, Dunn, and Simantob (1989)

92. A centrifuge modeling study conducted in three phases was performed for this investigation by personnel of the Department of Civil, Environmental, and Architectural Engineering at the University of Colorado, Boulder, CO. The first phase of the centrifuge modeling study, described in Report 1 (Ko, Dunn, and Simantob 1989) of the series, was a feasibility study and detailed description of equipment available. The second phase, Report 2 (Ko, Dunn, and

Simantob 1989), was a description of the hydraulics and theory involved, as well as a discussion of a modeling of models study. The final phase described in Report 3 (Ko, Dunn, and Hollingsworth 1989) was an attempt to simulate the behavior of two prototype embankments which failed as the result of overtopping. The work from each of the three phases will be briefly summarized and discussed here.

Report 1

93. Report 1 is a general introduction where the problem of overtopping is described along with the centrifuge proposed for use, its capacity, and its accoutrements. In order to accomplish sustained overtopping, it was necessary to deliver a higher flow rate of water to the model than had been necessary previously; consequently the water conveyance system of the centrifuge had to be modified. Water used for this model testing was taken from the Boulder (Colorado) municipal water system and was "wasted" after a single pass over the centrifuge model, i.e., model overtopping water was not recirculated with its entrained sediment. Equipment to measure and document erosion and rate of erosion is described. Equipment included a still twin camera stereography system as well as a closed circuit video system.

94. The soils and model preparation techniques used for the investigation are discussed along with test procedures which were evaluated and modified as the program progressed. This phase of the work involved the demonstration of capability; the conclusions drawn, essentially, were that the available equipment was capable of performing the required experiments and it would be possible to properly evaluate erosion and its effects on overtopping. Experiments were performed and the results shown to be reproducible.

95. It was recommended that future research should consist of validating scaling laws by conducting a "modeling of models" study at three different gravity levels, 25 g, 50 g, and 75 g.

Report 2

96. In Report 2 an experimental program involving three rigid and three erodible model embankments is described. The rigid embankments were constructed of aluminum and used to evaluate flow quantity and measure resulting water velocities as well as to perform a modeling of models study to verify that linearity exists between model size and acceleration level for the material and configuration in question. Erodible embankment models were constructed of typical silts and clays and were used to evaluate and document

erosion in the scale models using three scaling ratios: 1/24th scale, 1/49th scale, and 1/71st scale for both rigid and erodible model embankments. In the discussion of experimental procedure in Report 2, the authors describe the system which delivers water to the centrifuge model in flight. It seems that the system is configured such that overtopping water had to turn 90 deg before entering the embankment flow section and "it was observed that this led to a narrowing of the flow width." This apparent distortion of the entrance condition may have caused some of the uncertainties and difficulties observed in the experimental results. For example, the modeling of models study showed that the dimensionless coefficient of discharge, which is the proportionality coefficient between flow and head over the broad-crested weir of the model embankment, was a function of g-level and, therefore, model scale ratio n. Theory would suggest that this coefficient should be independent of g-level and constant. Also the ratio of time in the model to time in the prototype should be $1/n$, that is

$$\frac{t_m}{t_p} = \frac{1}{n} \tag{6}$$

However, based on centrifuge model tests performed in the study, the ratio of time in the model to time in the prototype computed from the average rates of erosion in all tests performed (and assuming the validity of the modeling of models) is

$$\frac{t_m}{t_p} = \frac{1}{n^{1.38}} \tag{7}$$

It was determined that the exponent assumed different values at different scaling ratios. The indicated exponent on the scaling ratio n would suggest that factors significant to the problems under consideration have not been properly accounted for in the overall modeling system. However, it must be remembered that only a limited number of tests were performed in this series. Two tests were performed at the scaling ratio of $n = 24$, three tests at the scaling ratio $n = 49$, and two tests at the ratio $n = 71$. Variations in model preparation may have accounted for some of the discrepancies between actual model performance and how the model should have performed as predicted by theory. However, the authors point out that in all the models tested in this phase of the study, erosion started at the toe and progressed upward toward the crest, and this progression is what is usually observed in prototype structures.

Report 3

97. In Report 3, the authors attempted to accomplish three objectives. They were:

a. To model actual overtopping events. It was attempted to model two fairly well documented events, the Clarence Cannon and Bloomington Lake cofferdam overtopping failures.

b. To determine the effects of modeling in two dimensions versus modeling in three dimensions.

c. To study the effects of nonhomogenous embankment cross-sections on erosion.

The modeling of Clarence Cannon cofferdam consisted of four tests and was conducted at a scaling ratio of $n = 80$. Two tests were performed on models constructed of a sandy silt (tests 1 and 2) and two tests were performed on a plastic clay (tests 3 and 4).

98. The distorted water inlet condition described above under Report 2 had not been modified for the tasks of phase 3 and therefore a different exponent on the scaling factors was computed for these tests at $n = 80$. Two of the four tests conducted showed strongly nonsymmetric erosion patterns which may have been due to the inlet condition. The authors did not state whether erosion which developed during overtopping started as toe cutting in these tests. The procedure used to measure erosion was to repeatedly start the centrifuge, induce overtopping flow across the model for a given time interval, stop the centrifuge to make measurements of the material removed, then restart the centrifuge. This method of operation may have, in itself, influenced the results considerably.

99. The strongest conclusion which can be reached from the authors' description and analysis is that the sandy silt used in tests 1 and 2 is considerably more erodible than the plastic clay of tests 3 and 4. The sandy silt endured 7.8 and 5.87 hr of overtopping flow before breaching occurred in the first two tests whereas the plastic clay used for the models of the last

two tests sustained 30.3 and 20.44 hr of overtopping with minimal erosion damage. The overtopping times given are prototype time projected from observations of the centrifuge model and may be uncertain because different time scaling factors were computed for all tests. The time scaling factors were 1.6, 1.66, 1.37, and 1.28 for tests 1, 2, 3, and 4, respectively.

100. Modeling of the Bloomington Lake cofferdam similarly consisted of four tests on the same two soils at a scaling ratio of $n = 80$. Basically the same criticisms and conclusions are valid for Bloomington Lake cofferdam as for the Clarence Cannon cofferdam.

101. To determine the effects of modeling in two dimensions versus three dimensions, three-dimensional models were prepared and tested for comparison with the two-dimensional tests conducted during phase 2 and described in Report 2. The results of the comparison tests appeared to be inconclusive with the three-dimensional embankments eroding more rapidly and completely in some tests and less rapidly and completely in others. However, it must be remembered that, here too, a limited number of tests were performed. The conclusion reached by the authors was that the three-dimensional tests were more desirable and representative of a prototype situation since in the two-dimensional tests there was an interaction between the model and container walls (boundaries) which was not present in the three-dimensional models.

102. The final series of tests in the investigation were performed to study the influence of zonation in embankments. Two types of zoned dams were tested, one type was constructed with a blanket drain, the other with a toe drain. When the section containing the blanket drain was overtopped and erosion began, the loose blanket drain was removed in seconds leaving a void within the structure. Erosion then began at the toe and worked its way up the embankment causing failure very rapidly. The embankment section prepared with the rock toe behaved similarly; the cohesive downstream shell was removed quickly by the overtopping water after which the rock toe was immediately washed away.

Conclusions from Centrifuge Modeling Studies

103. From evaluations of the centrifuge modeling work performed by Ko et al. conclusions which are believed warranted are:

a. The distorted water entrance condition in the equipment may have voided some of the qualitative factors considered in the analysis.

b. Quantitative agreement was not observed between the centrifuge experiments and prototype structures in the attempts to model documented prototype failures. However, prototype soil was not used in the centrifuge models. Different soil types were substituted for the prototype material in the (authors stated) attempt to bracket prototype behavior rather than duplicate it.

c. Plastic cohesive materials tend to be more resistant to erosion from overtopping than nonplastic cohesionless materials.

d. Homogeneous structures tend to be more resistant to overtopping damage than do composite or zoned structures.

e. Failure/collapse conditions on centrifuge models in flight seem to be qualitatively similar to those observed in prototype structures, that is, erosion typically begins as toe cutting and works its way upslope and through the crest toward full breach.

PART V: FLUME MODELING

104. In flume modeling, a small-scale geometrically similar model is tested in a hydraulic flume under prototype (nonaccelerated) gravity. Although this modeling technique was not pursued (extensively) in this investigation it is a technique in which similitude may be satisfied between model and prototype for some conditions. However, it must be pointed out that difficulty will be experienced using this technique to model overtopping and erosion in earthen embankments because soil is a material whose stress-strain and strength behavior is internal stress dependent and erosive processes may also be. The state of stress in a small model will be very different from that in a full-size prototype structure. Since strength is dependent on state of stress in soil structures, the reaction between geometric conditions produced by erosion and structural strength may produce very different collapse mechanisms in model and in prototype. Ko, Dunn, and Simantob (1989a), for example, describe preliminary tests on scale model crushed rock embankments conducted in a 1-g field. In those tests it was observed that erosion began at the crest of the embankment and progressed down the slope toward the toe. In prototype structures subjected to overtopping, experience shows that erosion typically begins at the toe and progresses upslope, toward the crest.

105. Soils derive strength from a combination of friction (which is a function of stress level and therefore physical size) and cohesion (which is a function of soil particle size and mineralogy). If prototype soil is used in a small-scale flume model then the ratio of cohesive strength to frictional strength will be very different in model and prototype. In the approach to embankment modeling where prototype material is used in the scale model, there is likely no way of matching ratios of frictional to cohesive strength between model and prototype in a 1-g field. As a result, an inappropriate strength mechanism might produce a failure/collapse mechanism in the scale model which is totally different from that which would be observed in the prototype under the driving force of overtopping and the resulting erosion.

106. There are modeling approaches which will allow stress levels to be matched between model and prototype but they all involve very specific conditions which are difficult to achieve. For example, there were three configurations described by Gilbert, Hale, and Kim (1985) in which (gravity) stress level is matched between model and prototype. Two of these configurations

involved altering the gravity field (one in the centrifuge, the other involved testing in a gravity field less than 1 g); the third involved finding and using as the model material, a substance whose density is n times the prototype density, where n is the scaling ratio. This is called the modeling of dissimilar materials, and it is not likely to be useful for investigating overtopping in 1 g except at scaling ratios very close to unity, which is a limiting restriction in that the advantage of small-scale modeling is defeated. Flume models of embankments subjected to overtopping in a 1-g field are generally most appropriate when applied to noncohesive materials. For example, flume model studies are sometimes used to investigate problems involving riprap (Oswalt 1968). Prototype riprap typically consists of cobbles, boulders, or man-made structures which interlock; all of these materials must be considered cohesionless and all, when used as riprap, are intended to protect soft or erodible underlying material. Because of the cohesionless nature of riprap, the problem of mismatched cohesive to frictional strength ratios may largely be avoided in flume models, but sound modeling technique must nevertheless be practiced, otherwise failure mode between model and prototype may not correspond as in the example described by Ko et al. (1989a) given above. In the example of the crushed rock embankment described by Ko et al. the ratio between gravity forces (friction between particles) and the inertia forces produced by moving water may have been the modeling parameters which dominated the problem. Failure to match these force ratios (Froude numbers) violated similitude and led to a terminal (failure) condition in the model different from that observed in the prototype.

107. It is evident that in the investigation of a problem as complex as overtopping, it is unlikely that similitude will be exactly achieved at any scaling ratio except one to one. Properly designed flume model experiments may be useful to study the reaction between moving water and cohesionless soils but such studies do not represent the problem of greatest interest or importance in the area of embankment erosion since most embankments are constructed of cohesive soil (clay). The inability to match the ratio of frictional to cohesive strength between model and prototype structures in flume embankment studies is a serious problem. It cannot be overcome in 1 g and it severely limits the usefulness of this modeling technique.

PART VI: MATHEMATICAL ANALYSIS OF OVERTOPPING-BREACHING

108. Modeling an embankment breaching process is a problem involving hydrology, hydrodynamics, sediment transport, topology, and geomechanics. Several mathematical models have been proposed and developed over the last twenty or so years to allow simulation of embankment breaching. However, modeling requires idealization of the actual situation so that factors controlling the physical process in question may be described by a manageable set of governing equations. The validity of a model is controlled by the soundness and generality of its theoretical base along with the number of simplifying assumptions made, the ability to determine the physical parameters required to describe the process, and the accuracy of the solution algorithm. There is always a trade-off between complexity, manageability, accuracy, and efficiency for any given model.

109. One of the most important factors in the problem under consideration is water flow and how it is handled in the overall model. The models described in this work handled water flow either by broad-crested weir flow or by the St. Venant equations. In broad-crested weir flow, discharge is empirically related to head (fluid height) over the weir. The St. Venant equations are a set of hyperbolic nonlinear partial differential equations for which no general solution exists. The system may be solved numerically either by the method of characteristics, finite elements, or finite difference. These numerical methods are well developed and documented and will not be discussed here, but the St. Venant equation will be stated for completeness.

110. Water flow through a receiving channel can be described in one dimension by two partial differential equations derived by St. Venant in 1871 and named for him. They consist of an equation for the conservation of mass, given by

$$\frac{\partial Q}{\partial X} + \frac{\partial A}{\partial t} + q = 0 \tag{8}$$

and an equation for the conservation of momentum given by

$$\frac{\partial V}{\partial t} + V \frac{\partial V}{\partial X} + g \frac{\partial h}{\partial X} + g S_f + \frac{Vq}{A} = 0 \qquad (9)$$

where

Q = discharge, ft^3/sec

X = coordinate along the waterway, ft

A = cross-sectional area, ft^2

t = time, sec

q = lateral outflow per unit length of waterway, $ft^3/sec/ft$

V = mean velocity = Q/A, ft/sec

g = acceleration due to gravity, 32.2 ft/sec^2

h = water surface elevation above a datum, ft

S_f = friction slope estimated from a steady-flow empirical formula such as the Chezy or Manning equations, ft/ft

$= \dfrac{n^2 Q^2}{CA^2 R^{4/3}}$ (the Manning equation, for example)

n = Manning roughness coefficient

C = constant = $(1.486)^2$

R = hydraulic radius = A/(wetted perimeter), ft

111. The other mechanism which accompanies water flow to result in breaching of embankments is sediment transport, which consists of the processes of erosion, entrainment, transportation, deposition, and compaction of sediment. Sediment transport is a scientific discipline that has been developed on a semi-empirical basis mostly for use in describing the action of alluvial rivers.

112. Several investigators have attempted to develop a numerical model which could, once calibrated, properly predict the rate of breaching of an embankment during overtopping. Generally, the models are based on sediment transport equations and make very broad assumptions about embankment homogeneity and soil properties. Some of the models are reviewed here. Current work at the Agricultural Research Service, Stillwater, Oklahoma, and San Diego State University, San Diego, California (funded by the National Science Foundation), seeks to develop numerical models which will describe the erosion and breaching processes.

113. Flood routing involves the mathematical predictions of a flood wave propagating through a river system as a function of time and location within the system. As far as mathematical modeling is concerned, dam-breach flood waves are essentially identical to precipitation runoff flood waves except for certain distinctive characteristics of dam-breach flood waves.

- a. The dam-breach flood wave is usually many times larger than the precipitation runoff flood of record. Consequently discharge and stage data are usually not available for model calibration.
- b. The dam-breach flood wave has a very short time base, particularly from the beginning of rise to the peak.

As a result, a large magnitude peak discharge rapidly occurring dam-breach flood results in a wave having significantly greater acceleration components than that usually associated with a precipitation runoff flood wave.

114. Most of the dam breach flood models use arbitrary embankment breaching rates and geometries to describe breach development. This is one of the most imprecise assumptions made in flood routing models. The rate of breaching can be very important to downstream flood-stage forecasting, particularly for areas immediately downstream of the embankment, for small reservoirs, narrow downstream valleys, and highly erosion-resistant embankments. It should be pointed out that during overtopping, flow will be turbulent and supercritical. Once failure by slumping occurs, flow will induce dynamic pressure fluctuations. Therefore the simplistic approach of computing erosion due to tractive shear stress exerted by flowing water under steady uniform turbulent supercritical conditions will not be applicable (Perry 1982).

115. Some of the more notable numerical models which were developed over the years will be briefly described here. Basic principles and fundamental assumptions of each model will be given. These particular models were chosen because they show the striking evolution from the simple and empirical conceptual approaches of the 1950's to the powerful and sophisticated computer codes of the 1980's.

Wilkins

116. Although not directed toward predicting a rate of breaching for embankment dams, Wilkins (1956, 1963), in work extending from a 1956 study, discussed the stability of rock-fill dams as a function of overtopping and

seepage. In the 1956 laboratory study, transmissibility tests on cylindrical specimens of crushed dolerite stone with upward water flow were performed. Following an approach outlined by Taylor (1948) Wilkins proposed the equation

$$V_v = C\zeta^a m^b i^h \tag{10}$$

where

- V_v = average velocity of water through the voids (equal the discharge velocity divided by porosity)
- C = a composite shape factor
- ζ = viscosity of water
- m = hydraulic mean radius of the rock voids (for a given volume, the volume of voids divided by the surface area of the particles)
- i = hydraulic gradient
- a,b,h = empirical constants

All parameters have dimensions inches, pounds, and seconds. For clean crushed stone, Wilkins found Equation 10 to be

$$V_v = 32.9m^{0.5}i^{0.54} \tag{11}$$

where V_v is in inches per second and m is in inches.

117. Wilkins (1963) then used the 1956 study as background for an analysis of the stability of overtopped rock-fill dams. He showed that unreinforced rock-fill dams constructed at the angle of repose are unstable during overtopping and will fail along a deep sliding surface as soon as the voids are nearly filled with water, provided failure has not already occurred due to raveling of the downstream face or erosion across the crest. For cases where raveling and deep sliding are prevented by steel rod reinforcement and steel tiebacks, respectively, Wilkins devised a procedure for sketching flow nets for turbulent flow. From the flow nets, pore pressures were estimated for use in a Bishop sliding circle analysis. With model tests using 9-in.-high reinforced embankments of clean crushed dolerite gravel, Wilkins found good

agreement between a factor of safety predicted by Bishop's sliding circle analysis and stability behavior observed in his model studies.

Cristofano

118. One of the earliest documented attempts at modeling erosion and breaching of an embankment was by Cristofano (1966) at the Bureau of Reclamation. Several broad assumptions were made to derive an equation based on an iterative process relating the volume of water passing over the embankment in a specified time increment to the increase in breach section due to the erosion by this volume of water. The resulting enlarged breach flow section would allow a greater flow of water during the next time increment and additional erosion of the channel.

119. Assumptions made include:

- a. Embankment properties allow, for a given time increment, a direct and constant relation between volume of water overtopping and volume of embankment eroded.
- b. An initial notch exists where erosion will start and develop.
- c. The breach will be trapezoidal in section perpendicular to flow, with side slope approaching the material's angle of repose. This allows use of a weir formula for calculation of flow.
- d. Width and side slopes of notch are constant for the given time increment (usually several time increments).
- e. Length of bottom of notch for shear resistance purposes is from upstream edge of notch to where the notch bottom intercepts the downstream slope or foundation. The slope of the notch is equal to the developed angle of internal friction ϕ_d .
- f. Transport of material sloughing from notch sides is ignored.

120. The empirical equation (hereafter referred to as the Cristofano equation) is

$$\frac{Q_s}{Q_w} = Ke^{-x} \tag{12}$$

where

Q_s = volume of soil eroded in the chosen time increment

Q_w = volume of water going through the notch in the chosen time increment based on the broad-crested weir formula and defined below

K = a constant of proportionality; Cristofano used 1 and implied K would not vary appreciably from 1

e = the base of the natural logarithm

X in Equation 12 is defined as

$$X = \frac{b \tan \phi_d}{Hi} \tag{13}$$

where

b = base length of the bottom of the overflow channel (in the direction of flow) at any given time

ϕ_d = the developed angle of friction of the soil; Cristofano stated that $11 \leq \phi_d \leq 15$ deg

121. Once the initial embankment geometry (see Figure 22), water level, reservoir rating curve (head versus outflow), and required soil properties are known, an initial erosion depth D is chosen for an assumed notch location and width. This allows calculation of Q_s/Q_w. A time increment Δt is chosen for an increase in $D, \Delta D$. Cristofano and fellow workers recommended an initial Δt as small as one second. Q_w is then calculated using the Cristofano-recommended broad-crested weir

$$Q_w = CLH^{3/2}\Delta t \tag{14}$$

where

C = nondimensional coefficient of discharge; Cristofano used 2.9

L = width of the notch parallel to the embankment axis

H = depth of water from reservoir surface to the bottom of the upstream end of the notch

Q_s is determined from the increase in notch cross-sectional area and length of notch b.

122. The calculated Q_s/Q_w ratio is compared with the Q_s/Q_w ratio from the Cristofano equation. If the two ratios are not sufficiently close in agreement, different ΔD's and/or Δt's are chosen until acceptable

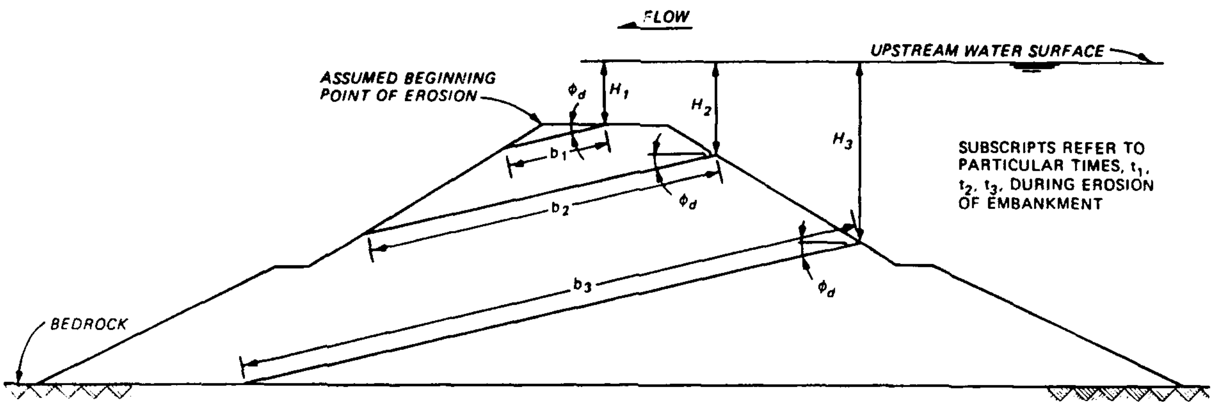

Figure 22. Geometry for Cristofano erosion model

agreement is reached. Subsequent ΔD's and Δt's are chosen and the same process is followed until the embankment is breached--provided there is enough water available. Variables such as notch width, soil properties, and head may be changed between time increments if desired.

123. This first step to numerically describe erosion and breaching of an embankment by overtopping has been accepted and used by many engineers developing flood models for dam failures. Little improvement has been accomplished since the introduction of this method. Nevertheless, several serious drawbacks to the Cristofano equation are evident:

- a. Case histories have shown that compacted earth embankments can sustain flows for long periods (12-20 hr) without definitive notching.
- b. Erosive processes other than areal erosion or erosion of the notch bottom are taking place, e.g. head-cutting or undercutting of the downstream slope.
- c. Little is known about what threshold flow, either depth or duration, is required before erosion becomes substantial.
- d. Embankments, as a rule, are not homogeneous or isotropic; compaction, permeable and impermeable components, structures, geometric changes, and changes in materials will influence the erodibility of the embankment.

124. Cripe (1973) prepared a computer program based on the Cristofano equation. Newton and Cripe (1973) used this or a similar program to study what flow conditions would cause failure of the Watts Bar Dam earth embankment.

Harris and Wagner

125. Stating that Cristofano's formula and its assumptions were unrealistic, Harris and Wagner (1967) proposed an approach based on the empirical Schoklitsch Bed-Load Formula. This formula relates the movement of bed-load to:

a. Grain diameter.

b. Channel slope and breach dimensions.

c. Critical discharge.

d. Actual discharge.

Harris and Wagner found pictures from three dam failures which supported their hypothesis of a 90-deg parabolic-shaped breach (Figure 23). They compared actual and calculated erosion and discharge for two dam failures. Calculated discharges were within 7 percent of measured.

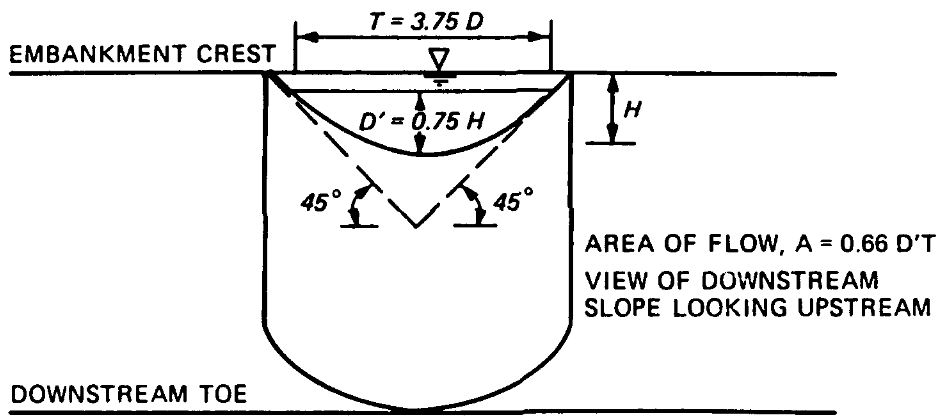

Figure 23. Breach configuration for Harris and Wagner hypothesis

126. Harris and Wagner made several simplifying assumptions:

a. Embankment properties allow, for a given increment of erosion, a direct and constant relation between volume of water overtopping and volume of embankment eroded.

b. The breach forms as a parabolic notch (Figure 23) and maintains this section.

c. The slope of the breach will be 5 to 20 deg.

The Harris and Wagner equation, while based on different variables, is of the same form as the Cristofano equation:

$$\frac{Q_s}{Q_w} = \frac{86.7\ S^{1.5}}{\sqrt{d}\ \gamma_s} \tag{15}$$

where

S = slope of the notch, the tangent of the slope angle (5 to 20 degrees)

d = average grain diameter, in.

γ_s = moist unit weight of soil, lb/ft^3

Equation 15 is based on the empirical Schoklitsch equation (Schoklitsch 1934) for bed-load coefficient.

127. As with Cristofano's method, embankment geometry, notch slope, water level, rating curve, and required soil properties must be known. An initial notch location and depth D are assumed. The ratio Q_s/Q_w for the Wagner and Harris equation is calculated. An initial incremental increase in depth ΔD is chosen. The initial ΔD should not exceed 5 percent of dam height, and subsequent ΔDs should be less than 10 percent of the initial dam height.

128. The initial ΔD is calculated and substituted into the Wagner and Harris ratio to determine Q_w . The increment of time Δt to erode the incremental depth ΔD is calculated by using a notch flow formula based on the equation for flow at critical depth in an open channel:

$$Q_w = \left(\frac{gA^3}{T}\right)^{1/2} \Delta t \tag{16}$$

where

g = acceleration of gravity

A = cross-sectional area of flow

T = width of flow at the water surface

Δt = flow time increment

A parabolic breach was assumed, and based on the properties of a parabolic section (see Figure 23)

$D = 0.75\ H$

$T = 3.75\ D$

A = 0.66 DT

Harris and Wagner developed from Equation 16,

$$Q_w = 5.54\ H^{5/2} \Delta t \tag{17}$$

or

$$\Delta t = \frac{Q_w}{5.54\ H^{5/2}} \tag{18}$$

where H is the depth in feet of water from the reservoir surface to the bottom of the upstream end of the notch (see Figure 24). Q_w must be expressed in cubic feet per second and Δt will be calculated in seconds. The rate of breaching and the outflow hydrograph can be determined from Equations 17 and 18.

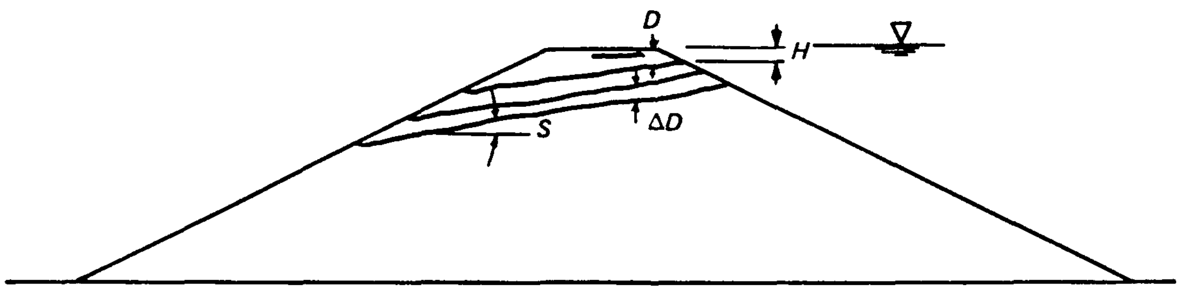

Figure 24. Cross section of notch for Harris and Wagner hypothesis

129. Though based on different variables, the Harris and Wagner equation has the same drawbacks as the Cristofano equation. Brown and Rogers (1977) used the Harris and Wagner procedure to back calculate the failure of Teton Dam due to breaching though the actual failure was due to piping. Computed erosion rates could not be compared with actual erosion rates of the dam since estimates of embankment removal rate were not available.

Wiggert and Contractor

130. A general hypothesis which considered the effect of erosion on embankment stability was developed by Wiggert and Contractor (1969). They were concerned that while the sediment transport approach could describe the areal or notch erosion of an embankment, a catastrophic failure might occur when only a portion of the embankment cross section had been removed. The failure would be caused to some degree by decreasing soil strength due to increased water content but primarily by changes in downstream slope geometry due to gulleying.

131. They proposed that the downstream embankment slope be divided into stations with depth and velocity at each station determined by methods of gradually varied flow in open channels. Manning's equation and the slope of the energy grade line would determine depth of flow. Shear stress and erosion rate would be calculated for each station. The difference in erosion rate for each station would cause a variation in downstream embankment slope and affect slope stability which would be analyzed periodically during overtopping.

132. The authors realized that more than areal or sediment transport erosion would occur during overtopping, but admitted that analysis of the breaching mechanisms would require some very general assumptions without any basis in quantitative model or prototype experience.

Fread

133. Fread (1971) developed a numerical model for dam breaching and flood routing. He assumed a V notch with constant arbitrary angle ϕ, and its progression was determined by arbitrarily assigning a rate of movement to the bottom of the V notch. In later studies (1977, 1978, 1980, 1981) Fread performed extensive research on dam breach flood wave propagation using the computer program DAMBRK. This program allows the user a choice of rectangular, triangular, or trapezoidal breach shapes. Breaching proceeds after reservoir water level exceeds a certain specified value and the breach bottom enlarges at a predetermined linear rate. The program incorporates both broad-crested weir flow over the breach and flow through the spillway outlets. The program does not have the capability to include the effects of sloughing. In the studies performed by Fread, DAMBRK was applied to five historic and well

known dam-breach floods. Although the results after calibration were satisfactory, the model cannot be used for flood prediction because the model requires factors such as input (which can only be known after breach), failure time, and terminal size and shape of the breaches. Therefore the Fread model is useful for the estimation of a spectrum of possible flooding eventualities but not necessarily useful for predicting a precise probable event. In 1984, Fread presented an iterative numerical model based on broad-crested weir flow over the breach and quasi steady-state uniform flow along the downstream face of the embankment with the capabilities to handle tailwater effects (Fread 1984). In the model called BREACH, sediment transport is handled by the Meyer-Peter and Muller equation. Additionally this model has the capability to include the effects of tailwater buildup and slope stability (sloughing) but this aspect of the model is severely limited by the fact that the theoretical treatment of slope stability was to assume the behavior of dry soil. Erosion is handled in the model by assuming that the breach slope is parallel to the downstream face of the dam. The usefulness of the model is limited by the fact that the terminal breach width and the very uncertain value of the critical shear stress for the initiation of erosion must be supplied to the model.

134. BREACH was used to analyze the failures of the Teton Dam in Idaho and the Mantaro Dam in Peru and showed reasonable agreement with the actual failure. However, in both cases the terminal geometry of the failed structure was known and a reasonable estimate of critical shear stress was used to calibrate the model.

Chee

135. From a series of model studies of sand embankments, Chee (1978a,b) developed equations for two flow conditions:

- a. Overtopping with a constant reservoir water level.
- b. Overtopping with a constant discharge through the breach (discharge was controlled downstream of the breach).

The equation developed for constant reservoir water level (Chee 1978a) was

$$\frac{qs}{qc} = \frac{1}{60} K_1K_2K_3K_4 \left(\frac{g[D-0.5H]}{q_c^2}\right)^{1/20} \left(\frac{1}{[S_s - 1]}\right)^2 \left(\frac{D}{d}\right)^{1/8} \tag{19}$$

where

q_s = mean solids discharge per unit width

q_c = critical water discharge per unit width computed from the value of D

D = constant water depth upstream of dam, Figure 25

g = acceleration due to gravity

H = height of embankment, Figure 25

d = mean grain size

B = mean width of dam, Figure 25

S_s = specific gravity of grains

E = distance between channel bottom and dam crest before erosion, Figure 25

θ = angle of repose of embankment material

m = thickness of clay core

K_1 = a coefficient which is a function of θ

K_2 = a coefficient which is a function of H/B

K_3 = a coefficient which is a function of E/H

K_4 = a coefficient which is a function of m/H

The equation developed for constant discharge through the breach (Chee 1978b) was

$$\frac{q_s}{q} = \frac{1}{73} K_1K_2K_3K_4(S_s - 1)^{-2} \left(\frac{yc}{d}\right)^{1/8} \tag{20}$$

where

q = constant water discharge per unit width

yc = critical flow depth calculated from q

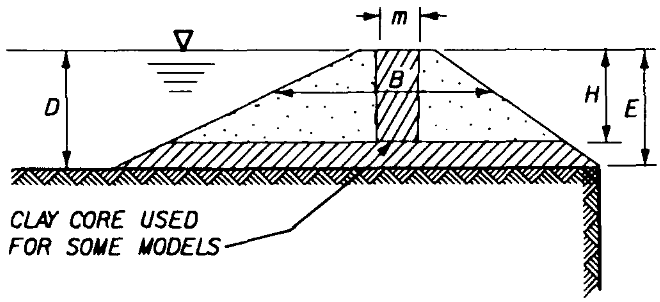

Figure 25. Embankment geometry (after Chee 1978a,b)

136. Time of breaching for both flow conditions is given by

$$t = V_{vol} \frac{(1-n)}{q_s} \tag{21}$$

where

t = washout time

V_{vol} = volume of embankment per unit width

n = porosity of embankment material

137. Chee's equations provided an average rate of embankment removal for the duration of breaching. Chee stated that the embankment eroded in three distinctive phases with different rates of erosion:

a. The initial phase consisted of rapid lowering of the crest with surface slips and back erosion causing flattening of the downstream slope.

b. A transitional phase where erosion continued as surface slip and bed-load transport. The overall erosion rate was much slower during this phase.

c. Finally, bed-load transport on a shallow slope continued at the slowest erosion rate.

138. Chee's work was concerned with predicting erosion rates for erodible fuseplug embankments placed in spillways in place of gates to allow passage of large floods. All the models were made of various size sands with different specific gravities. Certain models employed a central clay core.

Ponce and Tsivoglou

139. Though omitting details, Ponce and Tsivoglou (1981) described a numerical scheme based on sediment transport for modeling gradual dam

breaching. The method for the calculation of flow is based on the St. Venant system of equations. Ponce and Tsivoglou used the finite difference method to numerically solve the St. Venant system of equations. Breaching starts with an assumed rivulet which grows across the dam crest increasing in size and flow. Once the crest is crossed, flow and erosion increase more quickly. Breach width and flow rate are mathematically related but no details are given. The authors state that use of the Exner equation for sediment continuity and the Meyer-Peter and Muller equation for sediment transport were used to define a relation between sediment transport and mean velocity.

140. One example of a breached dam was modeled to verify the method. The dam, Huaccoto Natural Dam, Peru, was formed by a landslide and had very shallow slopes. The estimated actual and modeled values of erosion and discharge compared well though the authors state channel friction, sediment transport, and channel geometry were adjusted within physically realistic bounds.

141. The authors were contacted to determine if more details could be made available. More details were not available, but a research project funded by the National Science Foundation is being conducted by one of the authors to refine the model.

Lou

142. Lou (1981) explored three methods of calculating breaching and discharge rates for overtopped embankments, the fist two of which are based on St. Venant system of equation.

143. His first method used a combination of DuBoy's formula for transport of sediment in layers due to shear stress of flowing water and Einstein's approach for suspended load. Lou encountered numerical instabilities with this approach.

144. As his second method, Lou developed an equation for solid transport on the assumption that erosion is a function of kinetic energy which is measured by water velocity, time, and soil erodibility.

145. Finally, Lou used Cristofano's formula. He felt the equation for solid transport provided the best agreement with observed data for two dams: Teton and Mantaro. The Teton Dam failure was not due to overtopping and Mantaro Dam--apparently the same dam (Huaccoto Natural Dam, Peru) used by

Ponce and Tsivoglou (dimensions and general location are the same but dates differ)--was a landslide-formed dam with flat slopes (6H on 1V downstream) and uncompacted slide debris.

146. Lou concludes that the phenomenon is too complex for simple analysis with too many variables which make each overtopping situation unique. The many variables and lack of detail measurements make calibration of the models virtually impossible.

Simmler and Samet

147. As a result of modeling of homogeneous granular dams with and without impervious elements, Simmler and Samet (1982) proposed an equation to determine the ratio of water discharge to solids erosion:

$$\frac{Q}{G} = C_1 e^{C_2 E_z} \tag{22}$$

where

Q = water discharge through the breach, M^3/sec

G = erosion rate, M^3/sec

C_1, C_2 = coefficients which for cohesionless materials have the following limits

$$0.07 \leq C_1 \leq 0.2$$

$$3.0 \geq C_2 \geq 2.0$$

e = base of natural logarithm

E_z = an erosion ratio of final eroded breach volume to the uneroded breach volume at a particular time during the breaching process

A further note regarding E_z is appropriate. The premise of Equation 22 seems reasonable but it is based on limited model tests of granular materials; and final breach volume must be assumed to calculate E_2 values. The equation has essentially the same form as Cristofano (1966) with E_z being the only variable. The equation suggests that, with time, E_z will increase as breaching continues since the final eroded breach volume is a constant and the uneroded breach volume decreases with time (at a faster rate initially, then more slowly).

Future Outlook

148. Several models for predicting the rate of breaching of an overtopped embankment have been presented and discussed, each with its own advantages and limitations. When certain of the models are applied to well known, well documented historical dam failures, reasonable agreement with prototype behavior is realized, but this is partly due to the fact that there are parameters within each model which may be calibrated (or optimized) to improve the simulation. The effect of calibration/adjustment of parameter for better simulation (or fit) is apparent in that sloughing and tailwater are known to influence the discharge history and ultimate embankment geometry and yet none of the models except BREACH have the capability to handle sloughing and tailwater and the treatment (of sloughing) by BREACH is simplistically unrealistic. Yet by careful calibration of the models, reasonably good simulation is realized. In a true sense, none of the mathematical models are entirely satisfactory because the objective of modeling is to predict the outcome of a probable event from quantities which may be known at the onset of the event, such as geometry and material characteristics. This is not possible with existing models because those which do not require specification of an arbitrary breach geometry will require final breach dimension and uncertain (and often indeterminate) soil properties as input. Therefore, models to date, including the very sophisticated BREACH by Fread (1984), will only allow estimation of a spectrum of floods for different trial terminal geometries. Improvement of the existing state-of-the-art of modeling can be achieved by reducing the number of parameters within a model which need to be calibrated and by incorporating more realistic assumptions for water discharge and sediment transport mechanism into the models.

PART VII: MECHANISM OF OVERTOPPING

Overview

149. Embankment dam failure which occurs as a result of overtopping seldom begins with a catastrophic breach. Instead a series of progressive and interacting events occur which culminate in the breach. The total event is a combination of hydrologic, hydrodynamic, sediment transport, and geotechnical processes. Mathematically the process is an unsteady, nonhomogeneous, nonlinear three-dimensional problem which has not yet been formulated on a sound theoretical base. Although the dam breach process is mathematically quite complex, the physical prototype process has been observed and may be broken up into separate stages and described quite accurately along with the accompanying consequences. Lessons may be learned and conclusions drawn from the description of the process. The system in question is a two-phase soil-water interacting system where water from the reservoir first flows over the embankment crest until a notch is established then the notch enlarges by some combination of erosion and sloughing. The process continues until the reservoir is empty or until the embankment refuses further erosion.

150. Parameters which are thought to significantly influence the rate of events leading to breach are reservoir size and geometry, embankment size and geometry, embankment material and homogeneity, slope texture and smoothness, depth of overtopping, and the presence or absence of tailwater. In the following sections an embankment dam overtopping process will be dissected and the various stages discussed in chronological order.

Onset of Overtopping

151. This stage of the process in characterized simply by a rise in the reservoir level which can be rapid or slow. Four mechanisms named earlier which generally account for increased reservoir levels are sieches, slides into the reservoir, rainfall and rainwater runoff, or release from an upstream reservoir. The most frequently encountered cause of overtopping is flooding due to rainfall and rainwater runoff.

152. As the result of increased reservoir level (before overtopping ever occurs), two possible internal processes may occur to threaten the

stability of an embankment dam: (a) internal erosion due to piping and (b) erosion of the downstream face due to seepage. These two processes are aggravated by increased water level and may occur unobserved along with overtopping to result in the failure of a dam. The true objective of this work is to consider the isolated effect of overtopping, but such a consideration would be largely academic because in reality there will nearly always be some increased seepage occurring along with the actual overtopping to accelerate failure. Therefore, practically speaking, embankment dams are assaulted internally as well as externally by overtopping. In this light, one possible reason for the greater endurance to overtopping of homogeneous embankments constructed of highly plastic clays when compared to composite structures of lower plasticity materials is that homogeneous high plasticity dams are less susceptible to internal damage. High plasticity clays generally have low permeability and therefore are not as susceptible to seepage "blow out" and erosion as silts and sands of low plasticity. Because of the cohesive nature of highly plastic clays, these materials tend to be less erodible than similar materials of lower plasticity. It must be stated, however, that compaction of plastic clays at water contents above the optimum water content results in fills of reduced strength and designers must be aware of that fact, although the ability of such materials to deform without rupture may be worth the tradeoff in strength. Figure 26 illustrates the strength-deformation behavior of a cohesive material at various water contents with respect to optimum, and shows the characteristic brittle, high strength behavior at water contents below optimum and the low strength/plastic behavior above optimum.

153. The suggestion of this discussion is that other phenomena may combine with overtopping to result in the failure of an embankment dam, and that distress due to such mechanisms as seepage may begin before overtopping. The effect of these mechanisms may, in some cases, be minimized simply by manipulating the plasticity of the impermeable el nt of the dam to advantage. If the effect of mechanisms which act to damage an embankment dam internally could be minimized, then obviously the structures' resistance to overtopping would be increased.

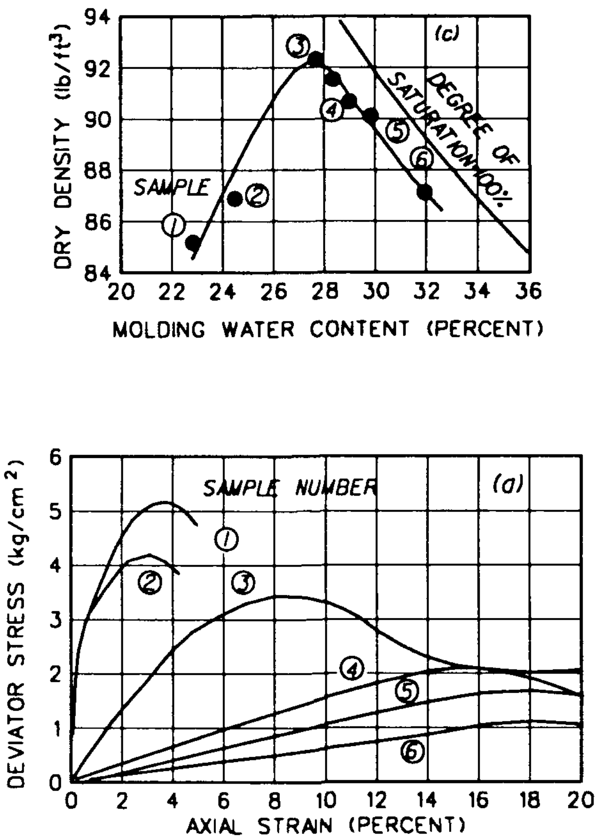

Figure 26. Stress-strain behavior of clay samples at different degrees of compaction (after Lamb and Whitman 1969)

Overtopping and Notch Development

154. At the onset of overtopping when water just begins to spill over the crest and flow down the downstream side of an embankment, depth is small and resistance to flow so high due to the proximity of the flow to a rough boundary that water does not gain significant velocity as it flows downslope. For example the Manning formula may be written in the form

$$V = \frac{1.49}{n} R^{2/3} S^{1/2} \tag{23}$$

where

V = average velocity at a cross section

n = roughness coefficient

R = hydraulic radius

S = slope of the bottom of the channel

and for wide, shallow, open channels such as flow over the crest of a dam the hydraulic radius R becomes approximately equal to the depth of flow. Therefore velocity varies directly with depth and for small depths, velocities are correspondingly small. However, the Manning equation describes a steady-state condition which is not maintained for long during an overtopping event where depth of overtopping continually increases. As water depth increases and losses decrease, energy considerations begin to dominate the problem and the vertical height through which water flows determines its velocity. For example a form of the energy equation is

$$V = \sqrt{2g\Delta z} \tag{24}$$

where

g = acceleration due to gravity

Δz = vertical distance between points on the slope

This equation completely neglects losses, and although losses decrease sharply as overtopping depth increases, losses are always present. However, the suggestion of Equation 24 is that the greater the vertical drop Δz, the greater will be the energy and momentum of water as it reaches the toe of the slope.

155. One additional factor which must be considered is that when water flows in a channel in steady turbulent incompressible flow, a shear stress is exerted on the channel walls which varies as the square of the velocity of flow, and is given by the equation

$$\tau_o = \tau \frac{\rho}{2} V^2 \tag{25}$$

where

τ_o = average channel wall shear stress

τ = a dimensionless coefficient related to channel roughness

ρ = mass density of fluid flowing

V = average water velocity

This shear stress, which is parallel to the bottom of the channel and in the direction of flow, is significant for soil-lined channels because when this stress becomes sufficiently large, particles will begin to be picked up and removed from the channel bottom. Chow (1959) presents the channel wall shear stress in a slightly different form as a unit tractive force given by

$$\tau_o = WRS \tag{26}$$

where

W = unit weight (density) of water

R = hydraulic radius

S = channel slope bottom

156. Channel wall shear stress and its evaluation are borrowed from open channel hydraulics, and obviously flow over an overtopped dam will not be as steady and controlled as that in a well designed open channel. However, many of the mechanisms acting in open channel hydraulics will be similar in flow over an embankment dam and certain conclusions may be drawn from open channel experience. For example, if one considers Figure 27, which contains a US Bureau of Reclamation (USBR) design recommendation for open unlined channels based on permissible tractive force (or average velocity) over noncohesive soils, the suggestions are that:

a. Resistance to erosion increases as average particle diameter increases.

b. Clear water is more abrasive and damaging to a soil slope than water with a sediment load.

For a similar evaluation of cohesive soil, Chow (1959) presents data determined from a USSR study (which is summarized in Figure 28) where tractive force (velocity) is presented versus material type and degree of compaction in a design chart. The suggestions are that:

a. Resistance to erosion increases as compaction increases.

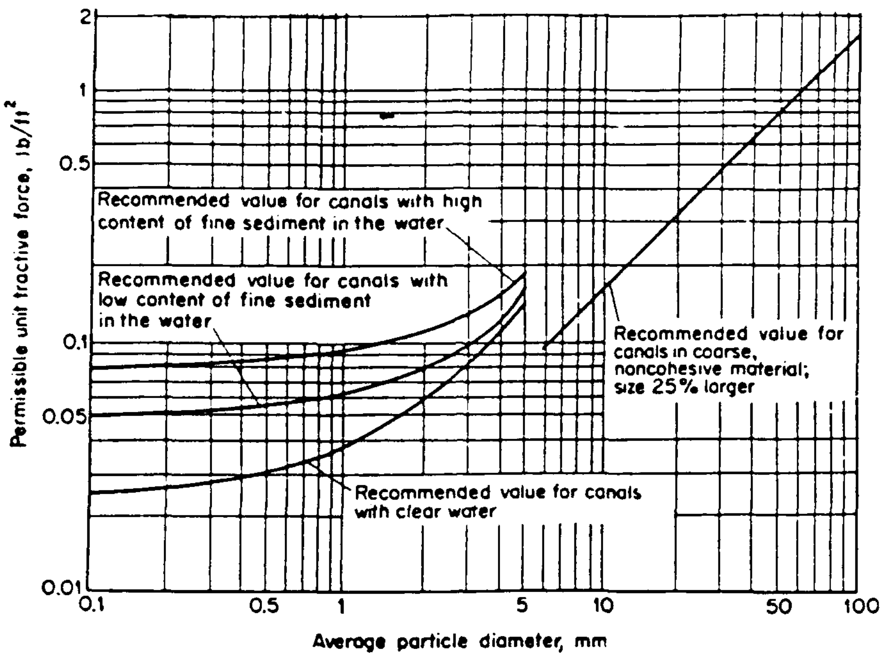

Figure 27. Recommended permissible unit tractive forces for canals in noncohesive material. (USBR)

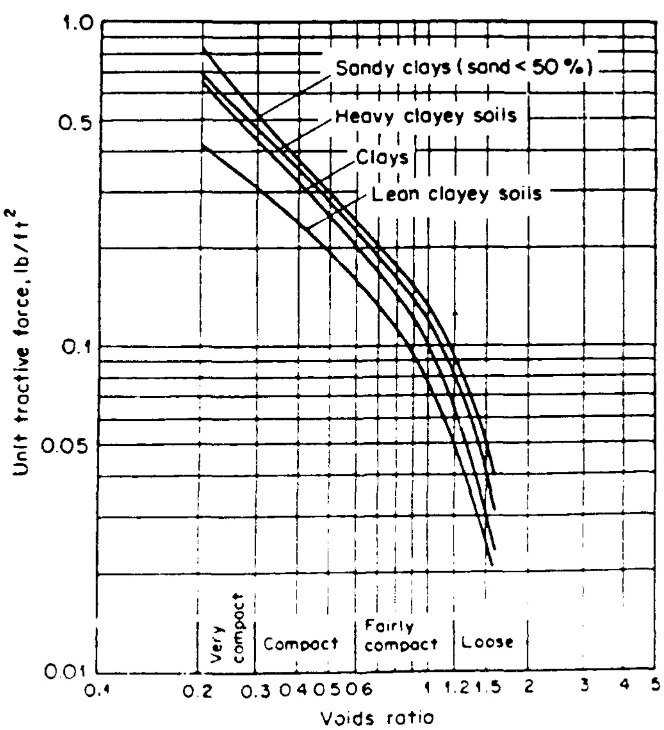

Figure 28. Permissible unit tractive forces for canals in cohesive material as converted from the USSR data on permissible velocities

b. Resistance to erosion increases as plasticity increases but a mixture of sand and clay offers the greatest resistance to erosion if the percentage of sand in the mixture is less than 50 percent.

157. Notch development begins as the threshold shear stress is exceeded and soil particles begin to move, initiating erosion. Logic would suggest that if vegetation were present on the downstream slope, the associated root system would reinforce the (slope) surface and delay the onset of erosion, but if the water velocity (and hence shear stress) were high enough to remove an entangled root system and the associated soil, then erosion of the underlying material would proceed quite rapidly. The effect of a root system would be to increase the strength of the material comprising the slope by increasing the apparent cohesion of the soil.

158. From data presented above taken from the study of related open channel hydraulics, it would appear that the speed with which erosion and notch formation will occur after overtopping is dependent on material character and strength (which in turn will depend on material compaction and surface texture), and the depth, velocity, and sediment load of water flowing over the slope. Obviously, if these characteristics were manipulated or controlled to advantage to maximize the threshold shear stress in a given embankment then the resistance of that embankment to overtopping would be increased.

Breach Development

159. Water flowing down the downstream face of the embankment gains energy and momentum and begins to move particles when a certain threshold velocity is exceeded. As water reaches the toe of the embankment the direction of flow changes abruptly as the slope changes from the steep slope of the downstream face of the embankment (which may be 25 to 33 percent) to the mild slope of the valley floor. Such an abrupt change in the direction of flowing water will result in the tendency for a hydraulic jump, and tremendous turbulence and energy dissipation which will likely cause damaging scour and erosion at the toe of the slope (Chow 1959). Material scoured and removed in this manner will oversteepen the downstream slope in the vicinity of the toe and will likely terminate with local slope failure due to some combination of:

a. Increased gravity stress due to oversteepening of the slope.

b. Excess pore pressure due to local shear strains.

c. Seepage pressures due to water flow-through.

d. Increased surface shear stress due to water flowing down the slope (see Equation 25).

160. The process is presented schematically in Figure 29. The first slope failure which occurs will leave a section of slope which is oversteepened. Water will now flow down this second slope with increased velocity and turbulence, erode into its toe, and oversteepen it in a manner exactly similar to that of the first slope. All the aggravating mechanisms (gravity stress, excess pore pressure, surface shear stress, etc.) will now combine to cause the second temporary slope to fail. The process will begin again on a third temporary slope, and in this manner will repeat as a series of successive slope failures which advance up the face of the downstream slope and through the crest. This process is very complex and unpredictable in that erosion and sediment transport continue along with the successive slope failures; there may be periods where erosion may be the dominant mechanism of material removal along with periods where slope failure or sloughing will appear to dominate material removal. It is also entirely possible that water currents may undermine sections of slope leaving them temporarily unsupported in the configuration of a cantilever beam. Such "beams" break off and are carried away as their unsupported length becomes too great. It is obvious that the process just described will follow a path of least resistance through the embankment if such a path exists. For example if there are zones of low plasticity and/or low compaction within an embankment, they would be more easily removed by flowing water from a matrix of well compacted plastic material causing geometric discontinuities which induce turbulence, promote material removal, and aggravate the breaching process. In this light, the value of homogeneity is seen in that in a homogeneous embankment, there is no path of least resistance.

161. Additionally, it must be mentioned that since seepage is occurring through the embankment, a flow net grid within a general embankment (see Figure 30) will show that the exit gradient is highest at the toe of the slope. A high exit gradient will tend to move soil particles as the result of internal flow; turbulence will tend to develop near the toe as the result of flowing water having to abruptly change direction because of the slope change at the toe. Seepage and turbulence will combine to create a worst case situation

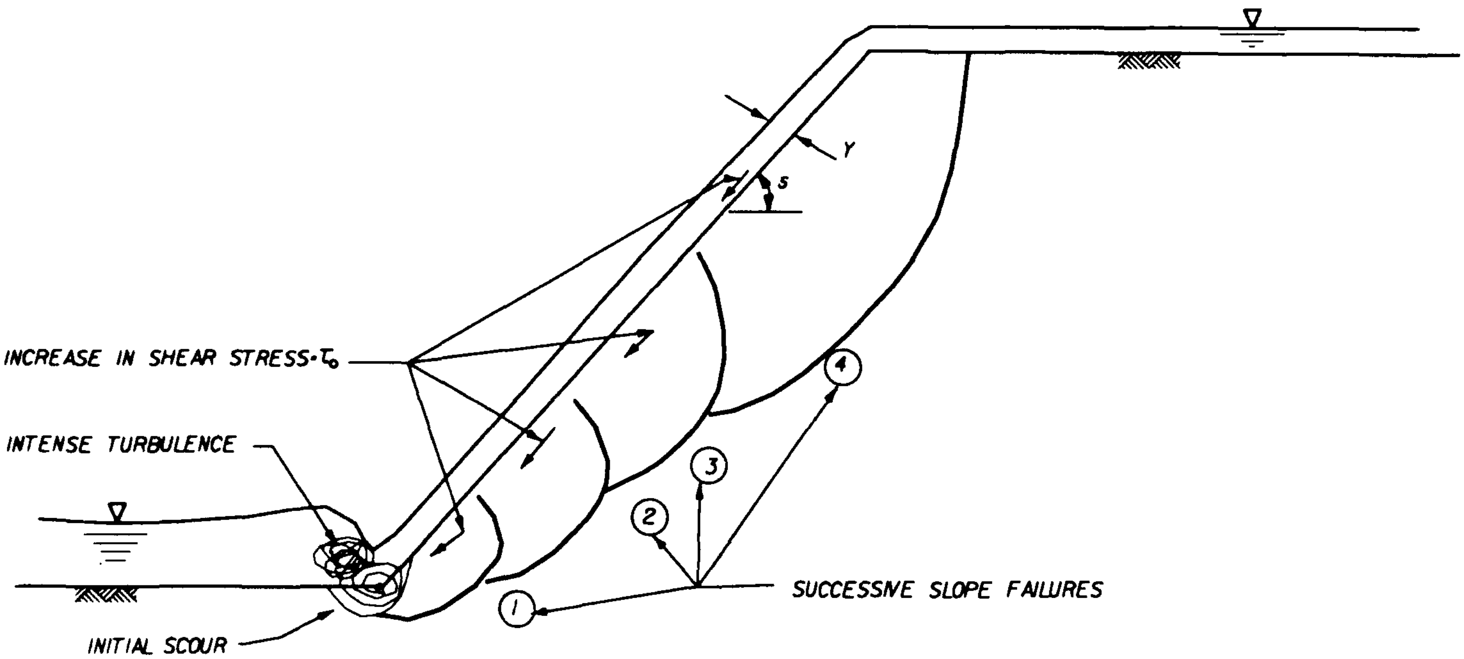

Figure 29. Schematic of successive local slope failures

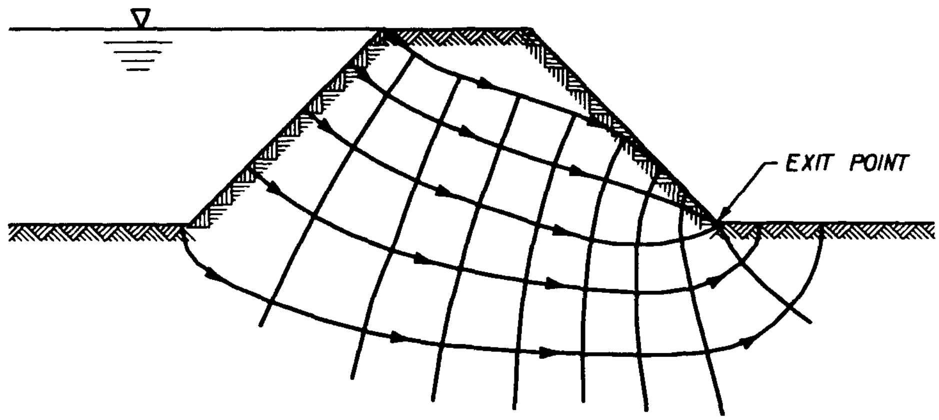

Figure 30. Flow net within embankment which is nearing overtopping

near the toe and may explain why erosion generally begins at or near the toe of the slope.

162. It should be pointed out that the process of breach development just described does not have to begin at the toe of an embankment. Any point along the downstream face of a dam where there is a discontinuity or an abrupt slope change is a potential point for the process to begin. As was mentioned in Part II, it appeared in the case of Rainbow Lake Dam, that overtopping flow channelized itself into ruts where "all-terrain" vehicles had worn away the vegetation, giving erosion a starting point. From the starting point, the breach process progressed and resulted in loss of the entire reservoir.

163. It should be noted that this process is not restricted to two dimensions in that sloughing and sliding can occur in a direction parallel to the longitudinal axis of the embankment as well as that perpendicular to it, and any direction in between. Slope failure perpendicular to the axis of the dam tends to widen the breach near the toe of the slope and gives the characteristic "fan" shape often observed. When the breach mechanism advances completely across the crest of the embankment, the breach will begin to deepen, increasing the area through which flow can occur and therefore the volume of flow as long as water is available from the reservoir. Increased flow will tend to scour and remove material from the established breach channel, further deepening the breach. Longitudinal sliding may then occur and result in widening of the breach as topology, quantity of flow, and material strength combine to reach a steady, terminal, equilibrium state. The problem then degenerates to one of steady-state flow in an open channel which may be described by Equation 26 which suggests that when a steady-state combination

of hydraulic radius (area of flow) and channel slope are established with the threshold shear stress of the channel material, no further erosion occurs. It should be noted additionally, that a breach does not always deepen all the way to the valley floor. Depending on quantity of water available from the reservoir and other factors, equilibrium may be established before complete destruction of the embankment occurs.

164. The presence or absence of a tailwater may also play an important role in breach development since kinetic energy of the flowing water could be dissipated and absorbed within and by a tailwater (if one were present) rather than reacting against a slope to scour away material there.

165. In a study to document cases of earth dam breaches, Ponce (1982) attempts to identify parameters in a prototype dam which increase overtopping resistance. Ponce observed that certain cases of non-engineered embankments with mild side slopes appeared to have increased resistance to overtopping and goes on to say that in cases where these structures were overtopped and ultimately failed, the breaching process may have lasted 24 to 48 hr and still not compromised the total embankment depth. These observations by Ponce may be consistent with the suggestions of this section that structures with mild side slopes appear to have increased resistance to overtopping. Mild side slopes will mean a less severe change in the direction of water flow at the toe of the slope and consequently less turbulence and erosion developing there.

PART VIII: DEFICIENCIES IN TECHNOLOGY

Deficiencies in Centrifuge Modeling

166. The fundamental processes of physical modeling in general and centrifuge modeling in particular were described in Part IV. Included in that part is a summary of and reference to preliminary centrifuge work performed during this investigation to evaluate the feasibility of using a geotechnical centrifuge to model and study behavior in overtopped embankments. Some of the advantages which may be gained by placing a small-scale model in the intensified gravity field of a centrifuge are discussed along with some of the significant uncertainties of the technique.

167. It was shown that good agreement between centrifuge model and prototype behavior can be expected only when similitude is achieved (between model and prototype), and this becomes very difficult when several phenomena occur simultaneously to form a resulting mechanism. Dam breaching is an example of several simultaneous phenomena combining to form a resultant failure mechanism and demonstrate the extreme difficulty in even formulating such a problem. The phenomena acting when a dam is overtopped and ultimately breached are open channel flow, seepage, sediment transport (including erosion as defined herein), and creeping (viscous) flow. It would not be difficult, in general, to achieve similitude between model and prototype with respect to any one of the aforementioned phenomena acting singularly. However, as these phenomena begin to occur simultaneously, it becomes difficult to the point of impossibility to completely satisfy similitude because these events occur at different time scales. Therefore, the effect of any one phenomenon on the terminal (failure) mechanism will either be exaggerated or diminished relative to the other acting phenomena. As time proceeds in the model, not only will the influence of any one phenomenon become increasingly distorted and incorrect (with respect to the prototype), but all the phenomena will interact with each other in an irreversible, progressive time dependent manner. Since the terminal (failure) mechanism will be determined by the time history of events in the process, there is no assurance that the terminal configuration of the model would be similar to the corresponding prototype configuration. In fact, logic would suggest that since the terminal prototype configuration is time history dependent, then the distortion of individual time history events in

the model would invariably lead to a terminal condition different from that in the prototype. What is additionally discouraging about the centrifuge modeling approach to this particular problem is that the distortion of time for various acting phenomena is size (acceleration level) dependent. Which is to say that events in time history would proceed differently at 1/70 scale (at an acceleration level of 70 g) than at 1/200 scale (at an acceleration level of 200 g), and therefore the terminal configuration will depend on the scale size under which the experiment is performed. On the other hand, it may be possible to design an experiment using the variable of scale model size to advantage, in that there may be a particular model size (acceleration level) which could be matched with a particular material particle size distribution and a dissimilar fluid to optimize the system and maximize similitude between model and prototype.

168. In centrifuge modeling, it is usual to select a model material whose particle sizes are not scaled in the exact geometrical sense. Either the unaltered prototype material is selected (for convenience) or another gradation with some desirable quality is selected, but seldom is the material properly scaled because it may be physically impossible to achieve the correct gradation without altering some other important material property such as strength or stress-strain response. Therefore void size and phenomena associated with void size and shape (such as seepage) will not scale correctly between model and prototype. The use of a fluid with a properly designed viscosity would facilitate such a problem, but the fluid would also need the proper sediment transport characteristic with respect to the chosen model material, and sediment transport consists of erosion, particle entrainment, particle transportation, particle deposition, and material compaction. It would be virtually impossible to find a fluid with the proper viscosity to simulate all of the processes of sediment transport precisely. However precise simulation may not be necessary. It may be enough to manipulate fluid viscosity along with other parameters to simulate some of the more important sediment transport processes in order to improve similitude. The best solution to this very complex problem will probably be found by optimizing similitude by the appropriate manipulation of (a) model size/acceleration, (b) material grain size distribution, and (c) viscosity of flowing fluid, and by calibrating the resulting model against well known and well documented historical prototype events. Additional research in this area is certainly

needed and may indicate the need for preliminary centrifuge studies in order to choose a model size/model material combination for actual centrifuge model studies.

Deficiencies in Numerical Models

169. Several numerical models have been presented and described in relative detail earlier in this work. The models ranged from a modest and hardly more than conceptual effort by Cristofano in 1965 to the very sophisticated BREACH computer model by Fread in 1984. The approaches to hydrodynamic flow in the models examined were based on either broad-crested hydraulic weir relations or the St. Venant flow equations. The sediment transport mechanisms utilized in the models were either based on empirical relationships or a steady fixed boundary system such as the Meyer-Peter and Muller bed-load formula. Even though these models represent significant advancement in the state-of-the-art, they fall short of their goal which is to predict precise single-event behavior of an overtopped embankment system from known geometric, topologic, and soil strength parameters.

170. The problem in modeling a phenomenon such as embankment overtopping is that it is very complex and consists of a number of separate phenomena acting and interacting together. The problem is highly indeterminate involving unsteady water flow as well as movable boundaries. The solution of such a problem would involve solving separately the unsteady (gradually varied, rapidly varied) water flow problem and the movable boundary problem, then combining the two solutions in a mathematically consistent manner together with the notions of effective stress and slope stability from geomechanics. Presently available analytical sediment transport treatments are developed from the standpoint of steady uniform flow with fixed boundary conditions; these assumptions are made for mathematical expedience and result in a significant departure from reality. A sound theoretical basis for unsteady sediment transport has not yet been formulated. The problem of sloughing and slope stability during an overtopping event would be difficult because not only would dynamic pore pressures due to seepage have to be included in the slope stability analysis, but the problem would have to be formulated in three dimensions because sliding in the embankment could potentially occur in any direction. Present numerical models which require calibration and a prior

knowledge of terminal breach geometry and size are of limited usefulness because they can only forecast a spectrum of possible response. Without the proper calibration parameters, soil properties, and terminal geometry, present models cannot predict the outcome of a specific probable event. To summarize, an improved numerical model would contain a minimum number of parameters which need to be calibrated and one which incorporates realistic water flow and sediment transport methodology.

171. The goal of any numerical modeling technique is to predict the behavior of full-size structures. Ultimate confirmation of a numerical modeling technique comes when predicted behavior matches that observed in a full-size structure. Full-scale tests of geotechnical structures are expensive and rare but scaled tests in a centrifuge are less expensive and, comparatively, many may be run to confirm and "fine tune" or calibrate a numerical model. However, a model test (such as a centrifuge test) itself may have to be calibrated against a well studied and documented prototype event. The solution to the very complex embankment overtopping problem will be achieved when correlation between numerical modeling, scale modeling, and prototype behavior is achieved.

172. Numerical modeling or computer analysis, being the most economical, would be the most desirable to use routinely. And because of the economy of such analysis, many eventualities and scenarios could be investigated. However, such a model must be founded on a sound theoretical base and should be calibrated against actual system behavior. Only by correlating and calibrating all three methods will full confidence in the approach and solution to the problem be fully established.

PART IX: CONCLUSIONS

173. Based on information acquired and lessons learned from study of prototype dams subjected to overtopping, centrifuge model studies of overtopped embankments, and study of numerical modeling techniques, all considered earlier in this work, the following conclusions are believed justified:

- a. If an unprotected embankment structure is overtopped by a sufficiently high head of water and the overtopping continues for a sufficiently long period, the structure will suffer varying degrees of damage by erosion which may lead to failure and complete breach of the embankment.
- b. The damaging effect of overtopping water is directly related to the head (height) of water above the crest of the embankment.
- c. The presence of a tailwater will lessen the damaging effects of overtopping flow.
- d. Erosion rate will be increased by seepage water discharging from the downstream slope. Erosion by seepage will be more severe in embankments constructed of silts and sands than in those of plastic clays.
- e. Embankment structures may be protected from overtopping damage by providing adequate emergency spillway capacity to handle floodwater likely to occur during the life of the structure.*
- f. Vegetation cover increases the erosion resistance by providing an initial protective cover and increasing the (apparent cohesive) strength of the surface of the downstream slope by root system reinforcement.
- g. Homogeneous (monolithic) soil structures tend to have greater resistance to overtopping than composite structures possibly because differential erosion and, hence, geometric discontinuities will result when two or more materials react with moving water associated with overtopping. Geometric discontinuities will aggravate turbulence and accelerate erosion.
- h. Incomplete embankment structures which consist of zones of dissimilar materials are especially susceptible to erosion damage for the reason stated in g. Protection provided by a completed structure is not present during construction with exposed discontinuities providing the potential for greatly accelerated erosion during overtopping. In areas and during periods of high risk to overtopping, provision should be made to protect incomplete structures with a temporary emergency spillway.

---

* It is recommended that all new embankment structures be designed and constructed with an adequate emergency spillway for the design life of the structure and, where risk analysis would dictate, existing structures be retrofit with an adequate emergency spillway.

i. Prototype case studies suggest that compacted earth embankments can resist overtopping flow for 10 to 20 or more hours without definitive breaching. As an example, Bloomington cofferdam breached in about 10 hr. The embankment was a homogeneous clayey sand with some gravel.

j. Flat (downstream) slopes are not as susceptible to damage from overtopping flow as are steep slopes.

k. Geometric discontinuities on embankment slopes can be starting points for turbulence and erosion if the slopes are exposed to water flow due to overtopping. Resistance to erosion damage will be enhanced if measures are taken to ensure that the (downstream) slopes are smooth and continuous.

l. Soil with a high plasticity index tends (in general) to have higher cohesive strength than a material with low plasticity index. Embankments constructed with highly plastic clay will tend to be more resistant to overtopping than those of lean clay or silt.

m. The problem of embankment overtopping is a very complex and important problem and one which causes extensive damage and property loss annually. The problem has not been adequately studied in terms of the analysis of prototype structures, or in terms of modeling techniques, either physical or numerical. All three areas show deficiencies in technology which can only be resolved by additional study and research. However, because of its complexity, embankment overtopping may be a difficult problem to resolve. Its complete solution, whenever it comes, will likely be a combination of numerical and physical modeling along with knowledge and experience gained from the study of prototype failures.

REFERENCES

Anonymous. 1976 (Jul). "Field Study of Emergency Spillway Performance During Southeast Kansas Storm on July 2 and 3, 1976," USDA Soil Conservation Service, Kansas.

__________. 1977 (Oct). "Brazilian Dam Failures: A Preliminary Report," Water Power and Dam Construction, Vol 29, No. 10, pp 51-53.

Baker, W. E., Westine, P. S., and Dodge, F. T. 1973. Similarity Methods in Engineering Dynamics, Spartan Books, Rochelle Park, NJ.

Brown, R. J., and Rogers, D. C. 1977 (Oct). "A Simulation of the Hydraulic Events During and Following the Teton Dam Failure," Proceedings of Dam-Break Flood Routing Model Workshop, Bethesda, MD, Water Resources Council, Washington, DC.

Budweg, F. M. G. 1982. "Safety Improvements Taught by Dam Incidents and Accidents in Brazil," Transactions of the Fourteenth International Congress on Large Dams, Q52, R73, Rio de Janeiro, Brazil.

Chee, S. P. 1978a (Jan). "Design of Erodible Dams," Proceedings of the International Conference on Water Resources Engineering, Vol 1, Fluvial and Coastal Hydraulics, Bangkok, Thailand.

__________. 1978b (Feb). "Mobile Controls for Water Resources Projects," Water Resources Bulletin, Vol 14, No. 1.

Chow, V. T. 1959. Open Channel Hydraulics, McGraw-Hill Book Company, New York.

Cook, L. A. 1986 (Dec). "Dam Failures During September 1986 Flood," Engineering-Water Management Division, Michigan Department of Natural Resources.

Cripe, M. W. 1973 (Nov). "Dam Breaching Program," Tennessee Valley Authority, Division of Water Control Planning, Knoxville, TN.

Cristofano, A. E. 1966. "Method of Computing Erosion Rate for Failure of Earth Fill Dams," Engineering and Research Center, Bureau of Reclamation, Denver, CO.

Daily, J. W., and Harleman, D. R. F. 1973. Fluid Dynamics, Addison-Wesley Publishing Company, Inc.

Fread, D. L. 1971. "Transient Hydraulic Simulation: Breached Earth Dams," Ph.D Dissertation, University of Missouri at Rolla, Rolla, MO.

__________. 1977 (Oct). "The Development and Testing of a Dam-Break Flood Forecasting Model," Proceedings of Dam-Break Flood Routing Model Workshop, Bethesda, MD, Water Resources Council, Washington, D.C., pp 164-197.

__________. 1978 (Aug). "NWS Operational Dynamic Wave Model, Verification of Mathematical and Physical Models in Hydraulic Engineering," Proceedings of the 26th Annual American Society of Civil Engineers Hydraulics Division Specialty Conference, College Park, MD, pp 455-464.

__________. 1980 (Mar). "Capabilities of NWS Model to Forecast Flash Floods Caused by Dam Failures," Proceedings of Second Conference on Flash Floods, American Meteorological Society, Boston, MA, pp 171-178.

Fread, D. L. 1981 (Oct). "Some Limitations of Dam-Breach Flood Routing Models," American Society of Civil Engineers Fall Convention, St. Louis, MO.

__________. 1984. "A Breach Erosion Model for Earthen Dams," National Weather Service Report, NOAA, Silver Spring, MD.

Gilbert, P. A., Hale, G. P., and Kim, Y. S. 1985 (Nov). "Identification of Geotechnical Parameters for the Physical Modeling of Retorted Oil Shale Piles," Department of Energy Report DOE/LC/11044-2071, Laramie, WY.

Harris, G. W., and Wagner, D. A. 1967 (Jun). "Outflow from Breached Earth Dams," Thesis for Bachelor of Science in Civil Engineering, University of Utah, Salt Lake City, UT.

Ko, H. Y., Dunn, R. J., and Simantob, E. 1989a (Apr). "Study of Embankment Performance During Overtopping and Flowthrough, Report 1, Feasibility Study," Miscellaneous Paper GL-89-5, US Army Engineer Waterways Experiment Station, Vicksburg, MS.

__________. 1989b (Apr). "Study of Embankment Performance During Overtopping and Flowthrough, Report 2, Hydraulic Study and Modeling of Models," Miscellaneous Paper GL-89-5, US Army Engineer Waterways Experiment Station, Vicksburg, MS.

Ko, H. Y., Dunn, R. J., and Hollingsworth, T. 1989 (Apr). "Study of Embankment Performance During Overtopping and Flowthrough, Report 3, Model-Prototype Comparison Studies," Miscellaneous Paper GL-89-5, US Army Engineer Waterways Experiment Station, Vicksburg, MS.

Lambe, T. W., and Whitman, R. V. 1969. Soil Mechanics, John Wiley and Sons, Inc., New York.

__________. 1982 (Jul). Proceedings of the Conference on Soil Dynamics and Earthquake Engineering, Vol 1, A. A. Balkema, Rotterdam, Netherlands, pp 367-378.

Linsley, R. K., and Franzini, J. B. 1979. Water Resources Engineering, Third edition, McGraw-Hill Book Company, New York.

Lou, W. C. 1981. "Mathematical Modeling of Earth Dam Breaches," Ph.D Dissertation, Colorado State University, Fort Collins, CO.

MacDonald, T. C., and Langridge-Monopolis, J. 1984. "Breaching Characteristics of Dam Failures," Journal of Hydraulic Engineering, American Society of Civil Engineers, Vol 110, No. 5.

Mitchell, C. H., King, E. C., and Rallison, R. E. 1966 (Jan). "Hydrologic Performance of Floodwater Retarding Structures During Colorado Storms of June 16-17, 1965," US Department of Agriculture, Soil Conservation Service, Denver, CO.

Newton, D. W., and Cripe, M. W. 1973. "Flood Studies for Safety of TVA Nuclear Plants, Hydrologic and Embankment Breaching Analysis," Tennessee Valley Authority, Knoxville, TN.

Oswalt, N. R. 1968 (Jun). "Riprap Protection for Subimpoundment Dams, Rend Lake Reservoir, Illinois," Miscellaneous Paper H-68-1, US Army Engineer Waterways Experiment Station, Vicksburg, MS.

Perry, E. B. 1982 (Jan). "Erosion Tests on Rock from Spillway at Lewisville Dam," prepared for US Army Engineer District, Fort Worth, US Army Engineer Waterways Experiment Station, Vicksburg, MS.

Ponce, V. M. 1982 (Aug). "Documented Cases of Earth Dam Breaches," SDSU Civil Engineering Series No. 82149, San Diego State University, San Diego, CA.

Ponce, V. M., and Tsivoglou, A. J. 1981 (Jul). "Modeling Gradual Dam Breaches," Journal of the Hydraulics Division, American Society of Civil Engineers, Vol 107, No. HY7, Proc. Paper 16372, pp 829-838.

Schoklitsch, A. 1934. "Der Geschiebetrieb und die Geschiebenfracht," Wasserkraft und Wasserwirtshoft, No. 4, p 37.

Scott, R. F., and Morgan, N. R. 1977. "Feasibility and Desirability of Constructing a Very Large Centrifuge for Geotechnical Studies," Report 760-170, National Science Foundation, Washington, DC.

Simmler, H., and Samet, L. 1982. "Dam Failure from Overtopping Studied on a Hydraulic Model," Transactions of the Fourteenth International Congress on Large Dams, Q.52, R.26, Rio de Janeiro, Brazil.

Taylor, Donald W. 1948. Fundamentals of Soil Mechanics, John Wiley and Sons, New York.

US Army Engineer Waterways Experiment Station. 1961 (Nov). "Floods Resulting from Suddenly Breached Dams--Conditions of Minimum Resistance," Miscellaneous Paper 2-374, Report 2, Vicksburg, MS.

US Department of Agriculture Soil Conservation Service. 1983 (Jan). "Performance of Floodwater Retarding Structures Elm Fork of Trinity River Watershed During October 1981 Storm, Temple, TX.

Whitman, R. V., Lambe, P. C., and Kutter, B. L. 1981. International Conference on Recent Advances in Geotechnical Earthquake Engineering and Soil Dynamics, Vol III, University of Missouri at Rolla, Rolla, MO, pp 1105-1110.

Wiggert, J. M., and Contractor, D. N. 1969. "Methodology for Estimating Embankment Failure," Report to Water Resources Engineers, Inc., Department of Civil Engineering, Virginia Polytechnic Institute, Blacksburg, VA.

Wilkins, J. K. 1956 (Jan). "Flow of Water Through Rockfill and Its Application to the Design of Dams," Proceedings of the Second Australia-New Zealand Conference on Soil Mechanics and Foundation Engineering, Canterbury University College, Christchurch, New Zealand.

__________. 1963 (Aug). "The Stability of Overtopped Rock-Fill Dams," Proceedings of the Fourth Australia-New Zealand Conference on Soil Mechanics and Foundation Engineering, University of Adelaide, Australia.

Wustemann, G. 1960. "The Breaching of the Oros Earth Dam in the State of Clara, North-East Brazil," Water and Water Engineering, Vol 64, No. 774.